THE JOURNAL OF BIOLOGICAL CHEMISTRY VOL. 285, NO. 13, pp. 9881–9897, March 26, 2010

In Vitro and *in Vivo* Enhanced Generation of Human A9 Dopamine Neurons from Neural Stem Cells by Bcl-X_L *[S]

Received for publication, August 10, 2009, and in revised form, January 15, 2010 Published, JBC Papers in Press, January 27, 2010, DOI 10.1074/jbc.M109.054312

Elise T. Courtois[‡], Claudia G. Castillo[‡§], Emma G. Seiz[‡], Milagros Ramos[‡], Carlos Bueno[¶], Isabel Liste[‡], and Alberto Martínez-Serrano[‡1]

From the [‡]Center of Molecular Biology Severo Ochoa (Consejo Superior de Investigaciones Científicas-UAM), Department of Molecular Biology, Autonomous University of Madrid, 28049 Madrid, Spain, the [¶]Institute of Neurosciences, University Miguel Hernandez of Elche, 03550 Alicante, Spain, and the [§]Department of Biochemistry, Faculty of Medicine, University of San Luis Potosí, 782 San Luis Potosí, México

Human neural stem cells derived from the ventral mesencephalon (VM) are powerful research tools and candidates for cell therapies in Parkinson disease. Previous studies with VM dopaminergic neuron (DAn) precursors indicated poor growth potential and unstable phenotypical properties. Using the model cell line hVM1 (human ventral mesencephalic neural stem cell line 1; a new human fetal VM stem cell line), we have found that Bcl-X_L enhances the generation of DAn from VM human neural stem cells. Mechanistically, Bcl-X_L not only exerts the expected antiapoptotic effect but also induces proneural (*NGN2* and *NEUROD1*) and dopamine-related transcription factors, resulting in a high yield of DAn with the correct phenotype of substantia nigra pars compacta (SNpc). The expression of key genes directly involved in VM/SNpc dopaminergic patterning, differentiation, and maturation (*EN1*, *LMX1B*, *PITX3*, *NURR1*, *VMAT2*, *GIRK2*, and dopamine transporter) is thus enhanced by Bcl-X_L. These effects on neurogenesis occur in parallel to a decrease in glia generation. These *in vitro* Bcl-X_L effects are paralleled in *vivo*, after transplantation in hemiparkinsonian rats, where hVM1-Bcl-X_L cells survive, integrate, and differentiate into DAn, alleviating behavioral motor asymmetry. Bcl-X_L then allows for human fetal VM stem cells to stably generate mature SNpc DAn both *in vitro* and *in vivo* and is thus proposed as a helpful factor for the development of cell therapies for neurodegenerative conditions, Parkinson disease in particular.

Parkinson disease (PD)[2] motor symptoms arise from the progressive degeneration of dopaminergic neurons (DAn). Experimental therapies, based on the cell replacement of the lost substantia nigra pars compacta (SNpc) DAn using human ventral mesencephalic (VM) fetal tissue provided proof of principle of a therapeutic effect of the transplants on a long term basis (1). However, in addition to ethical problems related to fetal tissue procurement, practical limitations were found, like the need for large amounts of VM tissue and the elevated cell death rate of the transplanted cells (2).

As an alternative, human neural stem cells (hNSCs) derived from the developing and adult central nervous system were initially used, but they were inefficient for DAn generation (3). Another stem cell source, the embryonic stem cells, required long and difficult differentiation protocols as well as neuronal and DAn progenitor selection to obtain high amounts of DAn (4, 5). Previous transplantation studies established that the generation of functional SNpc DAn *in vivo* was highly dependent on the regional tissue origin, the VM being the optimal region (6), and that only DAn with SNpc properties (meaning adequate patterning, transcription factor, and differentiated protein profile) were able to reinervate the striatum and induce a therapeutic effect (7). Therefore, human fetal VM-derived cell strains were established (8, 9), but their use was hindered by a limited and unstable DA differentiation potential (10) (as it was previously described for rodent and human VM neurospheres (11, 12)) and DA-related oxidative stress (13).

To the human cell lines of VM origin previously reported (8, 14), we have recently contributed a new immortalized human fetal VM NSC line (hVM1), which shows a great potential for the generation of SNpc DAn *in vitro* (15). In the present work, we have aimed at increasing our understanding of key factors involved in phenotypical stability, DAn generation, and functional maturation both *in vitro* and *in vivo*.

* This work was supported by European Union Grants QLK3-CT-2001-02120 DANCE and CP-FP-214706-2 EXCELL, Spanish Ministry of Science and Technology Grants SAF2001-0841 and SAF2004-03405, Spanish Ministry of Science and Innovation Grant BIO2007-66807, Carlos III Institute of Health Grant RETICS TerCel RD06/0010/0009, La Caixa Foundation Grant BM05-22-0), and Comunidad Autónoma de Madrid Grant GR/SAL/0115/2004. This work was also supported by an institutional grant from Foundation Ramón Areces to the Center of Molecular Biology Severo Ochoa.

A. M. S. dedicates this work to Profs. J. Satrústegui and J. M. Cuezva, thanking them for continuous support and help.

[S] The on-line version of this article (available at http://www.jbc.org) contains supplemental Figs. S1–S5.

[1] To whom correspondence should be addressed: Center of Molecular Biology Severo Ochoa, C/ Nicolas Cabrera 1, 28049 Madrid, Spain. Tel.: 34-91-196-4620; Fax: 34-91-196-4420; E-mail:amserrano@cbm.uam.es.

[2] The abbreviations used are: PD, Parkinson disease; 6-OH-DA, 6-hydroxydopamine; DA, dopamine; Ab, antibody; DA-ergic, dopaminergic; DAn, dopaminergic neuron(s); FACS, fluorescence-activated cell sorting; GFAP, glial fibrillary acidic protein; GAPDH, glyceraldehyde-3-phosphate dehydrogenase; hNSC, human neural stem cell; IRES, internal ribosome entry site; JNK, c-Jun N-terminal kinase; LTR, long terminal repeat; NAC, *N*-acetylcysteine; NSC, neural stem cell; PI, propidium iodide; rhGFP, *Renilla raniformis* humanized green fluorescent protein; DAT, dopamine transporter; SNpc, substantia nigra pars compacta; TH, tyrosine hydroxylase; VM, ventral mesencephalon; Z-, benzyloxycarbonyl; fmk, fluoromethyl ketone; PBS, phosphate-buffered saline; GABA, γ-aminobutyric acid; Q-RT, quantitative reverse transcription; HPLC, high performance liquid chromatography; hNSE, human neuron-specific enolase; hNu, human nuclei; ANOVA, analysis of variance; ICC, immunocytochemistry.

Bcl-X_L (basal cell lymphoma-extra large) belongs to the Bcl-2 (B-cell lymphoma 2) protein family, playing an important anti-apoptotic role in mammals (16), particularly during central nervous system development (17), but also modulating neuronal differentiation (18–21).

Our results demonstrate that Bcl-X_L enhances the maintenance of the neuronal and dopaminergic competence in long term expanded cultures and protects the cells from apoptotic cell death during differentiation. Bcl-X_L modulates fate decisions, increasing neuronal and dopaminergic differentiation by a dose-dependent mechanism, in parallel with a decrease in glial cell generation. Finally, we demonstrate that hVM1-derived cell lines survive transplantation in a rat model of PD, differentiating into neurons and glia and generating mature DAn, and that Bcl-X_L enhances functional recovery of Parkinsonian rats.

EXPERIMENTAL PROCEDURES

Cell Culture

Cell isolation and immortalization were described previously (15). Briefly, human ventral mesencephalic cells were isolated from a 10-week-old aborted fetus (Lund University Hospital). Tissue procurement was in accordance with the Declaration of Helsinki and in agreement with the ethical guidelines of the European Network of Transplantation. Immortalization was carried out by infection with a retroviral vector coding for *v-myc* (LTR-vmyc-SV40p-Neo-LTR) (22). Cells were routinely cultured on 10 μg/ml polylysine-pretreated plasticware in epidermal growth factor and basic fibroblast growth factor (20 ng/ml each; R&D Systems)-supplemented chemically defined medium (Glutamax (Invitrogen), 1% Albumax (Invitrogen), 50 mM Hepes (Invitrogen), 0.6% glucose, N2 supplement (Invitrogen), 1× nonessential amino acids, penicillin/streptomycin, Dulbecco's modified Eagle's medium/F-12 medium), referred to hereafter as "proliferation medium." To induce cell differentiation, cells were seeded at 10^5 cells/cm^2 in proliferation medium (in poly-L-lysine-treated plastic wells or coverslips). After 24 h, proliferation medium was replaced by differentiation medium (without epidermal growth factor and basic fibroblast growth factor and containing 1 mM dibutyryl-cAMP (Sigma) and 2 ng/ml human recombinant glial cell-derived neurotrophic factor (Preprotech)) (8). Differentiation medium was changed every second day until the end of the experiment. Cells were proliferated and differentiated at 37 °C and 95% humidity in a low oxygen atmosphere (5% O_2, 5% CO_2, in a dual CO_2/O_2 incubator (Forma)).

Generation of Bcl-X_L-overexpressing hVM1 Cell Sublines

The generation of stable Bcl-X_L-overexpressing hVM1-derived cell lines was done as previously described (19). Briefly, the hVM1 polyclonal cell line (15) was infected at passage 6 with a Bcl-X_L coding (LTR-Bcl-X_L-IRES-rhGFP-LTR) or empty (LTR-ø-IRES-rhGFP-LTR) retroviral vector at a multiplicity of infection of 1 particle/cell. After infection, the cells were selected by fluorescence-activated cell sorting (FACS), yielding three stably transfected polyclonal cell lines: hVM1-ø (control cell line), hVM1-low Bcl-X_L, and hVM1-high Bcl-X_L (expressing low and high rhGFP). rhGFP fluorescence levels correlated well with Bcl-X_L protein levels (see Fig. 2). Cell lines were routinely cultured under standard conditions as described before.

Immunocytochemistry (ICC)

Cells were fixed in freshly prepared 4% paraformaldehyde, PHEM (Pipes, Hepes, MgCl), 4% sucrose, except for neurotransmitter detection, for which 0.1% glutaraldehyde-supplemented 4% paraformaldehyde was used. Fixed cells were blocked for 1 h in PBS containing 10% normal horse serum, 0.25% Triton X-100 and incubated overnight at 4 °C with monoclonal antibodies against tyrosine hydroxylase (TH) (1:1000; Sigma), β-III-tubulin (1:1000; Sigma), glial fibrillary acidic protein (GFAP) (1:1000; Sigma), or dopamine (DA) (1:1000; Fitzgerald)) or polyclonal antibody against TH (1:1000; Chemicon), β-III-tubulin (1:1000; Sigma), GFAP (1:1000; Dako), γ-aminobutyric acid (GABA) (1:6000; Sigma), glutamate (1:10,000; Sigma), 5-hydroxytryptamine (1:1000; Sigma), G-protein-regulated inward rectifier K^+ channel (GIRK2) (1:400; Alomone), Pitx3 (1:500; Chemicon), or apoptosis-inducing factor (1:50; Cell Signaling). Afterward, cells were rinsed and incubated with secondary antibodies: Cy5-conjugated Ab (anti-mouse or anti-rabbit (1:500)), Cy3-conjugated Ab (anti-mouse or anti-rabbit (1:200), all from Jackson Immunoresearch), biotinylated anti-mouse (BA2001, 1:250; Vector Laboratories), biotinylated anti-rabbit (BA1000, 1:250; Vector Laboratories) antibodies, or AMCA-conjugated Avidin compound (1:500; Vector laboratories). Cell nuclei were counterstained with Hoechst 33258 (Molecular Probes; 0.2 mg/ml in PBS) or with TO-PRO (1:1000; Invitrogen).

Western Blotting

Cells (proliferating or differentiated) were harvested using trypsin/EDTA (Invitrogen), washed twice with PBS, and resuspended in lysis buffer (1% Triton X-100, 150 mM NaCl, 20 mM Tris-HCl, pH 7.5, 0.5 mM EDTA, 1 mM EGTA) in the presence of protease inhibitors (complete mini-EDTA free protease inhibitor mixture tablets, Roche Applied Science) for 30 min at 4 °C and centrifuged at maximum speed 20 min at 4 °C. Protein concentration in the supernatants was determined using the Bradford protein assay (Bio-Rad). 10–20 μg of protein were separated in a 10% SDS-polyacrylamide gel and transferred to a nitrocellulose membrane. Blots were then incubated overnight at 4 °C with monoclonal antibodies against β-actin (1:5000; Sigma) or polyclonal antibody anti-En1 (engrailed1) (1:500; Santa Cruz Biotechnology, Inc. (Santa Cruz, CA)), anti-synapsin-I (1:200, Chemicon); anti-Bcl-X_L (1:1000; BD Transduction Laboratories), anti-activated caspase-9 (1:500; Alexis), anti-β-III-tubulin (1:1000; Sigma), or anti-TH (1:1000; Chemicon). Secondary antibodies were used at 1:10,000 (Bio-Rad) for peroxidase anti-mouse Ab and 1:5000 for peroxidase anti-rabbit Ab (Vector). Immunoreactivity was detected using the ECL Western blot detection system (Amersham Biosciences) and quantified by scanning densitometry using Quantity One software (Bio-Rad).

Flow Cytometry Determinations

Fragmented DNA—Proliferating or differentiated cells were trypsinized and fixed overnight in 70% ethanol at −20 °C, and

stored at −20 °C until analysis. At the time of analysis, cells were incubated for 30 min at 37 °C in the staining solution (PBS containing 0.1% sodium citrate, 0.3% Nonidet P-40, 0.02 mg/ml RNase, and 0.05 mg/ml propidium iodide (Sigma)). DNA content was determined using a fluorescence-activated cell sorter, the FACSCalibur flow cytometer (BD Biosciences). A total of 10.000 events were acquired per sample using CELLQuest software (BD Biosciences), and the sub G_0-G_1 fraction (fragmented DNA) was quantified by Flowjo software. Samples were run in triplicate.

Analysis of Cell Viability by Annexin-V Binding and Propidium Iodide Staining—Alive cells were directly stained in the culture dishes by adding Annexin-V binding buffer and Cy5-conjugated Annexin-V according to the manufacturer's instructions (Annexin-V apoptosis detection kit, ABCAM) for 5 min in the dark. Afterward, cells were harvested by tripsinization, centrifuged, and resuspended in Annexin-V buffer. Propidium iodide (PI) (1 μg/μl; Sigma) was added to the cells, which were then analyzed in a FACS flow cytometer (FACSCalibur, BD Biosciences), using the FL-2 channel for PI detection and the FL-4 channel for Cy5-Annexin-V detection. Annexin-V binds to the membrane aminophospholipid phosphatidylserine, which is externalized from the inner to the outer leaflet of the plasma membrane in the early stage of apoptosis. When membrane integrity is lost, as seen in the later stage of cell death resulting from apoptotic process, PI staining becomes positive. Ten thousand events were acquired and analyzed using the Flowjo software. Apoptotic cells were defined as Annexin-V^+/PI^-- and Annexin-V^+/PI^+-stained cells. Necrotic cells were defined as Annexin-V^-/PI^+ cells.

Activated Caspase-3 Detection—At the specified time points, cells were harvested (including cells floating in the supernatant), washed with PBS-staining solution (2% bovine serum albumin, 0.01% NaN_3, 2% fetal calf serum in PBS), and incubated for 20 min at 4 °C with phycoerythrin-conjugated activated caspase-3 antibody (BD Pharmingen) (1:500) in PBS-staining solution containing 0.3% saponin in the dark. Afterward, the cells were washed and resuspended in PBS-staining solution plus saponin for FACS analysis. Data were acquired with CELLQuest software and analyzed using Flowjo software. Samples were run in triplicate, and at least 10,000 events were collected for each one.

Mitochondrial Inner Membrane Potential ($\Delta\Psi_{mit}$)—Cells were incubated with the Mitoprobe™ $DiI_1C(5)$ assay kit (Molecular Probes) for 30 min at 37 °C in PBS. After rinsing with PBS twice, propidium iodide (1 μg/ml in PBS) was added, and cells were incubated for 15 min before analysis using a 633-nm excitation laser and filtering the emission at 660/13 nm (FL-4 channel). PI was analyzed as previously. Positive controls for depolarized mitochondria were obtained using an uncoupler (carbonyl cyanide 3-chlorophenylhydrazone) or after apoptosis induction with camptothecin.

RNA Extraction and Real-time Q-RT-PCR

Total RNA was isolated from proliferating or differentiated cells using the High Pure RNA isolation kit (Roche Applied Science) according to the manufacturer's instructions. To proceed from rat tissue, rat brains were quickly removed from anesthetized animals and stored in RNAlater (Ambion) at −20 °C until RNA extraction. Total RNA was isolated using the RNeasy Lipid Tissue Midi kit (Qiagen).

The cDNA was synthesized from 1 μg of RNA using the High Capacity cDNA Achieve kit (Applied Biosystems). Relative quantification (RQ) of mRNA expression was performed by TaqMan real-time PCR using the commercial probes described below (TaqMan® gene expression assays, Applied Biosystems), according to the manufacturer's protocol on an ABI PRISM 7900 HT sequence detection system. Probes were as follows: Neurogenin2, *NGN2* (Hs 00702774_s1); NeuroD1, *NEUROD1* (Hs 00159598_m1); mouse achaete scute complex homolog I, *MASH1* (Hs 00269932); LIM homeobox transcription factor 1b, *LMX1B* (Hs 00158750_m1); Engrailed-1, *EN1* (Hs 00154977_m1); paired-like homeodomain transcription factor 3, *PITX3* (Hs 00374504_m1); nuclear receptor-related 1, *NURR1* (or *NR4A2*) (Hs 00428691_m1); tyrosine hydroxylase, TH (Hs 00165941_m1); dopamine β-hydroxylase, *DBH* (Hs 00168025_m1); vesicular monoamine transporter, *VMAT2* (or *SLC18A2*) (Hs 00996837_m1); dopamine transporter, *DAT* (or *SLC6A3*) (Hs 00168988_m1); *CALRETININ* (Hs_00158423_m1), *β-III-TUBULIN* (Hs_00964962_m1); *GFAP* (Hs 00157674_m1); *GIRK2* (or KCNJ6) (Hs 00158423_m1); *18 S* RNA (Hs99999901_s1); and human *GAPDH* (Hs 99999905_m1). To standardize the amount of sample cDNA added to the reaction, we used the amplification of endogenous controls human *GAPDH* or *18 S* rRNA. The fluorescence threshold and detection cycle of each sample/target gene was determined using ABI Prism SDS software (Applied Biosystems). The $\Delta\Delta Ct$ method was used to calculate the relative transcript abundance of a given gene. Gene expression was expressed as the -fold change between relative transcript levels in a calibrator sample (hVM1-ø proliferating/transplanted cells) compared with a sample of interest (differentiated/transplanted cells or other cell type). All cellular experiments were run in triplicate. For *in vivo* Q-RT-PCR, probes used were previously tested for their specificity to human RNA, not cross-reacting with rat RNA (except for 18 S rRNA, which amplifies both).

DA Determination by High Performance Liquid Chromatography (HPLC)

hVM1 cells were plated onto 10 μg/ml polylysine-pretreated dishes. For extracellular DA determination, 500 μl of the incubation medium (Hanks' balanced salt solution) was collected and added to a tube containing 125 μl of 1 M perchloric acid (Merck) with antioxidants (0.2 g/liter $Na_2S_2O_5$ (Merck), 0.05 g/liter Na_2-EDTA (Merck)) on ice. Samples were then centrifuged at 15,000 rpm for 20 min at 4 °C. For intracellular DA content determination, proliferating or differentiated cells were harvested and collected into Eppendorf tubes containing 100 μl of 0.1 M perchloric acid with antioxidants (see above) on ice. Samples were then sonicated briefly and centrifuged at 15,000 rpm for 20 min at 4 °C. Supernatants and cell extracts were then stored at −20 °C until analysis. DA was assessed using HPLC with electrochemical detection, as described previously (23). Samples were directly injected into the HPLC system (50 μl) without dilution or further purification.

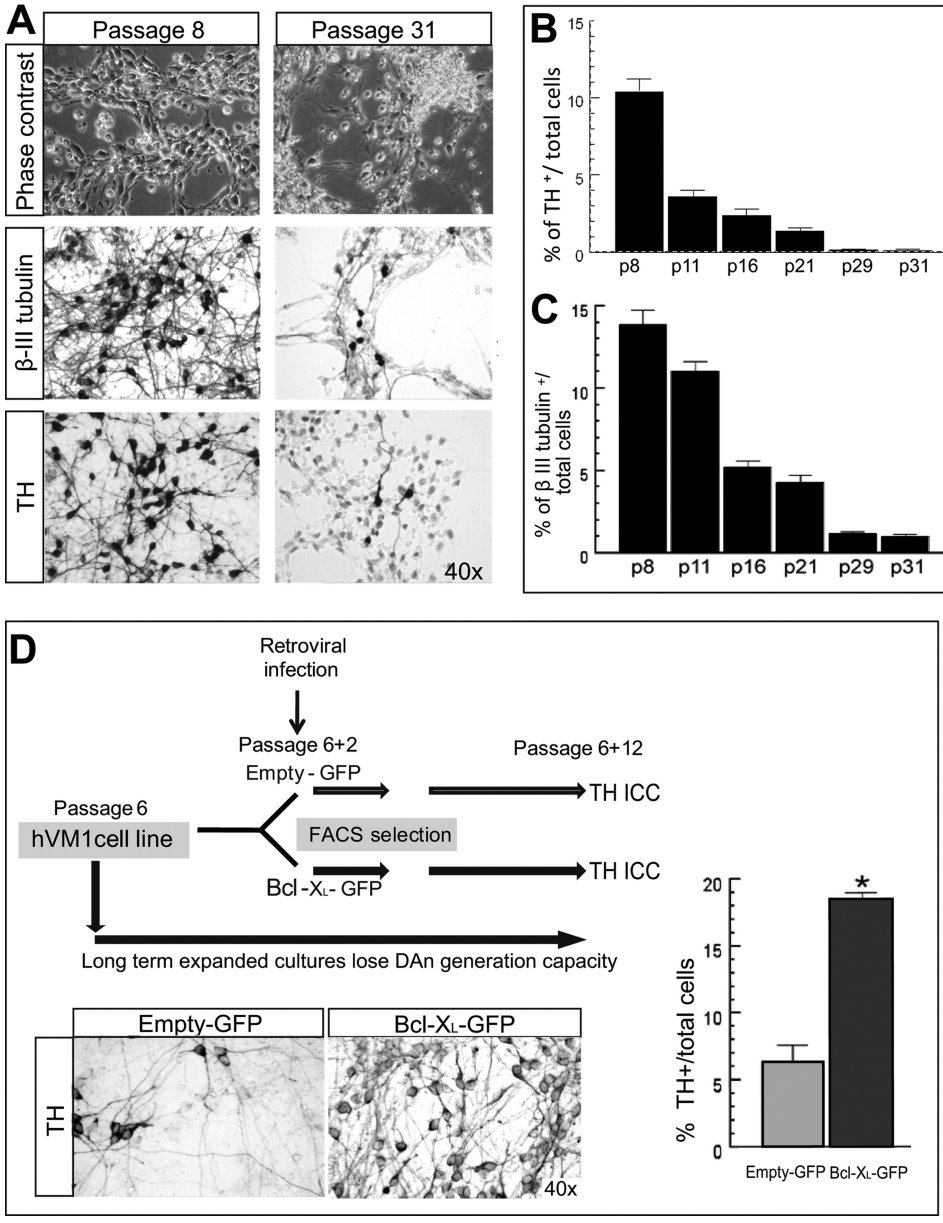

FIGURE 1. **Neuronal and dopaminergic differentiation in long term expanded hVM1 cells; effect of Bcl-X_L overexpression.** *A*, phase-contrast photomicrographs of 7-day differentiated cells at passages 8 and 31 (or the equivalent of one and a half years in culture). Differentiated cells were stained for β-III-tubulin and TH by ICC. *B* and *C*, percentage of TH^+ and β-III-tub^+ cells in differentiated hVM1 cells proliferated from passage 8 to 31. Data represent mean ± S.E. ($n = 3$). *D*, schematic of the short term experiment to study Bcl-X_L effects on the maintenance of the potential for TH^+ neuron generation. For this purpose, hVM1 cells were infected with a retroviral vector coding for Bcl-X_L (*Bcl-X_L-GFP*) or an empty vector (*Empty-GFP*) at passage 6, sorted by rhGFP fluorescence, and then expanded for 12 more passages. At this time point, cells were differentiated and analyzed for TH^+ cell generation. Microphotographs show TH staining. The *graph* represents the percentage of TH^+ cells.

Animal Experimentation; Lesion, Transplantation Procedures, and Drug-induced Rotation

Experiments were carried out according to the guidelines of the European Community (Directive 86/609/ECC) and in accordance with the Society for Neuroscience recommendations. Animals used in this study were 3-month-old female Sprague-Dawley rats (Harlan), weighing 200–250 g at the beginning of the experiment, housed in a temperature- and humidity-controlled room, under 12-h light/dark cycles, with *ad libitum* access to food and water. Rats received a 6-hydroxydopamine (6-OH-DA) injection (9 μg/3 μl dissolved in 0.9% saline containing 0.2 mg/ml ascorbic acid; Sigma) in the right median forebrain bundle at the following stereotaxic coordinates (tooth bar set at −3.3 mm) (24): anteroposterior, −3.7 mm; mediolateral, −1.6 mm (both from bregma); dorsoventral, −8.8 mm from dura. The injection rate was 1 μl/min, and the syringe was kept in place for an additional 5 min before being slowly retracted. Four weeks after the lesion, the rats were tested for rotational behavior in automated rotometer bowls (Panlab) following an injection of apomorphine (0.2 mg/ml; Sigma) and 1 week later with D-amphetamine sulfate (5 mg/kg, intraperitoneally (Sigma); for details, see Fig. 8). Rotational scores were collected every 2 min for 60 min for D-amphetamine test and 40 min for apomorphine test in a computer-assisted rotometer system (Panlab). Only rats exhibiting 5 or more ipsilateral rotations/min after D-amphetamine injection, and at least 4 contralateral rotations/min in response to apomorphine injection were selected for further transplantation studies. Hemiparkinsonian rats were then randomly assigned to two experimental groups, balanced for their rotation scores: (*a*) hVM1-ø cell transplant and (*b*) hVM1-high Bcl-X_L cell transplant. Cells for transplantation (in proliferative state) were dispersed and resuspended in Hanks' balanced salt solution (Invitrogen) at a density of 10^5 cells/μl. Medium or cell suspensions (3 μl) were injected into the denervated striatum at the following coordinates (in mm): anteroposterior, +1; mediolateral, −3; dorsoventral, −4.5 (from dura), with the tooth bar set at −2.3. The animals were immunosuppressed with daily intraperitoneal cyclosporin A injection (15 mg/kg; Novartis), starting 2 days before transplantation and throughout the experiment. Motor behavior was studied by D-amphetamine and apomorphine-induced rotation at 3 and 7 weeks after transplantation (for more details, see Fig. 8).

Immunohistochemistry

At the end of the experiment, the animals were anesthetized with an overdose of chloral hydrate and intracardially perfused

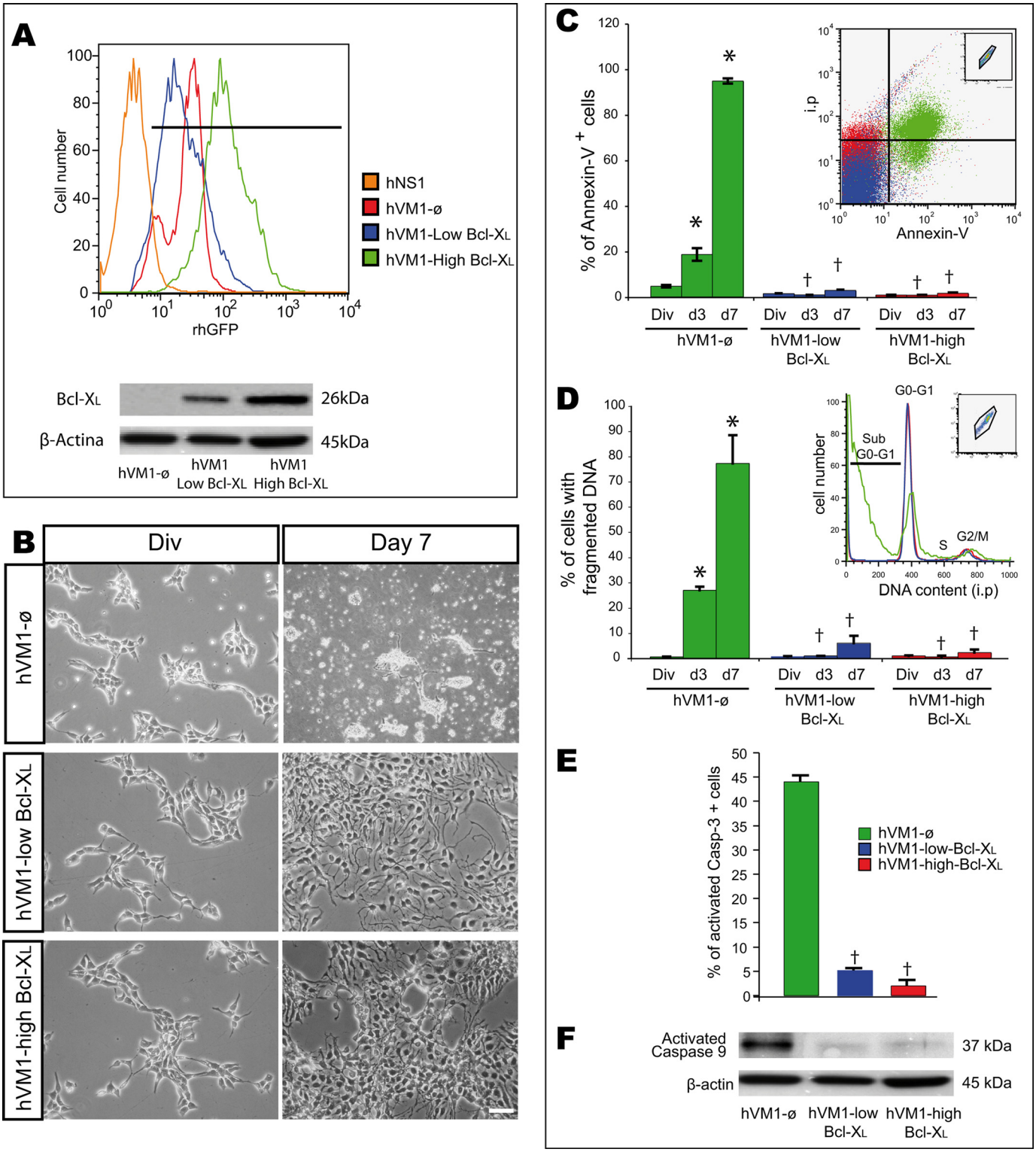

FIGURE 2. **Cell death in hVM1-derived cell lines; effects of Bcl-X$_L$ overexpression.** *A*, hVM1-derived cell lines were FACS-selected based on their rhGFP fluorescence after retroviral infection with LTR-ø-IRES-rhGFP-LTR or LTR-Bcl-X$_L$-IRES-rhGFP-LTR vectors, thus generating three polyclonal cell lines: hVM1-ø, hVM-low Bcl-X$_L$, and hVM-high Bcl-X$_L$. Forebrain-derived hNS1 cells (22) were used as negative control for GFP fluorescence. Overexpressed Bcl-X$_L$ protein levels (Western blot, *bottom*) did correlate well with rhGFP fluorescence (*β*-actin was used as a loading control). *B*, phase-contrast photomicrographs of proliferating and 7-day differentiated cells (passages 20–25). Note the massive cell death occurring in control cells with differentiation. *Scale bar*, 20 *μ*m. *C–E*, during differentiation, the cell death rate was determined by Annexin-V binding (*C*), DNA fragmentation (percentage of cells with sub-G$_0$-G$_1$ DNA content (*D*), and activated caspase-3-positive cells (at 7 days) (*E*) by FACS. Cells under proliferation conditions (control or Bcl-X$_L$-overexpressing cell lines) did not show any fragmented DNA or activated caspase-3 staining when analyzed. *Insets* in *C* and *D* illustrate FACS profiles of hVM1-ø, hVM-low Bcl-X$_L$, and hVM-high Bcl-X$_L$ cells when analyzed after 7 days of differentiation. All cell populations were first gated according to their size and complexity. Data represent mean ± S.E. of three independent experiments ($p < 0.05$, one- or two-way ANOVA, post hoc Tukey honestly significant difference test; †, *versus* hVM1-ø; *, *versus* day 0). *F*, Western blot of hVM1-ø- or Bcl-X$_L$-overexpressing cell lines after 7 days of differentiation stained to detect activated caspase-9. Blots were also double-stained for *β*-actin as a loading control.

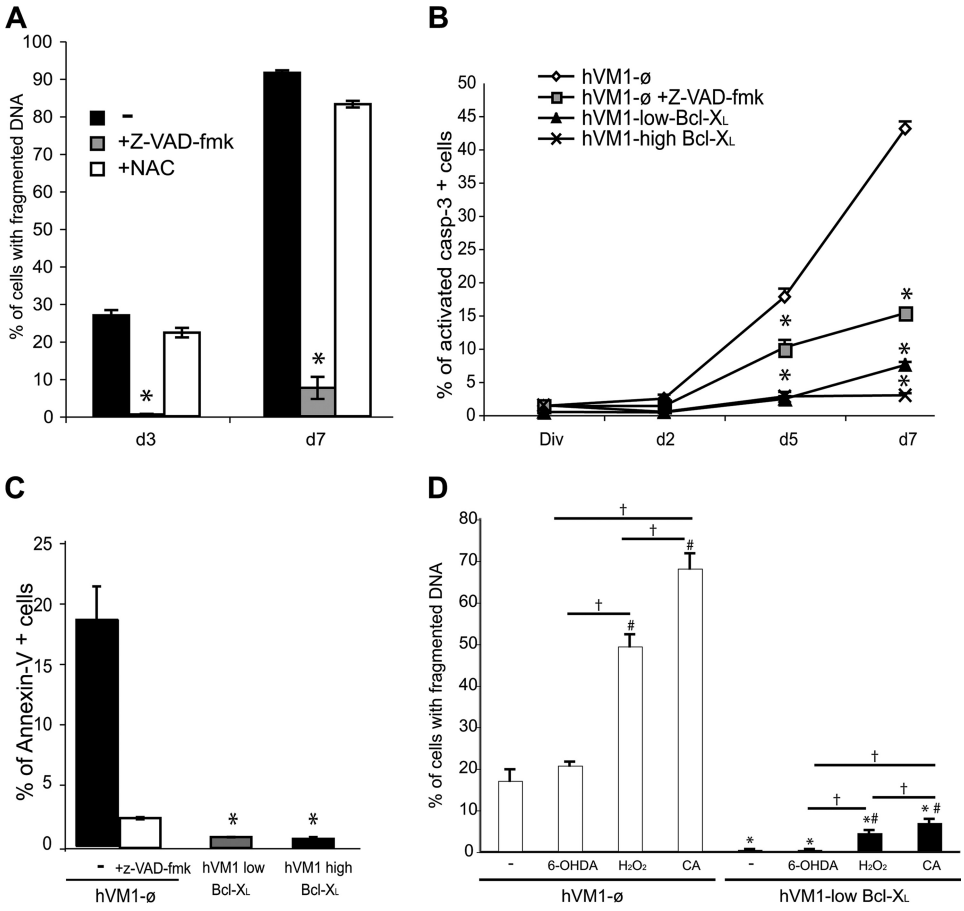

FIGURE 3. **Effects of Z-VAD-fmk, NAC, α-methyl-*para*-tyrosine, and cytotoxic agents (H_2O_2, 6-OH-DA, and camptothecin) on cell death during cellular differentiation.** *A–C*, effect of Z-VAD-fmk treatment on cell death in hVM1-ø cells during cell differentiation. *A*, fragmented DNA was determined in hVM1-ø cells when treated with 50 μM Z-VAD-fmk or 500 μM NAC since the beginning of the differentiation period. No differences were observed in Z-VAD-fmk- or NAC-treated Bcl-X_L cell lines when compared with non-treated ones (−). *B*, activated caspase-3 detection by FACS in hVM-ø (with or without Z-VAD-fmk), hVM1-low Bcl-X_L, and hVM1-high Bcl-X_L lines during differentiation. *C*, outer phosphatidylserine exposure detection by FACS (Annexin-V-positive cells) in 3-day differentiated cells. *D*, cell death was determined by DNA fragmentation in hVM1-ø and hVM1-low Bcl-X_L cells after 3 days of differentiation in the presence of 100 μM 6-OH-DA, 100 μM H_2O_2, or 40 μM camptothecin (*CA*). Data represent mean ± S.E. of three independent experiments. $p < 0.05$, ANOVA, post hoc Tukey honestly significant difference test; *, *versus* hVM-ø cells; #, *versus* no treatment; †, between treatments.

with freshly prepared, buffered 4% paraformaldehyde (in 0.1 M phosphate buffer, pH 7.4). Brains were removed, postfixed for 12 h in the same fixative at 4 °C, and dehydrated in 30% sucrose solution at 4 °C until sunk. Eleven 30-μm-thick coronal sections were collected using a freezing microtome. Serial sections were used for immunohistochemistry with polyclonal antibodies against TH (1:1000; Chemicon), DAT (1:1000; Chemicon), and Dcx (1:1000; Santa Cruz Biotechnology) and monoclonal antibodies against human GFAP (1:1000; Sternberger), human neuron-specific enolase (hNSE) (1:1000; Chemicon), or human nuclei (hNu) (1:100; Chemicon). Briefly, free-floating sections were incubated overnight at 4 °C with the primary antibodies diluted in PBS with 2% nonspecific serum. Sections were rinsed four times in PBS for a total time of 1 h and then incubated for 2 h with the secondary antibodies in PBS (see "Immunocytochemistry (ICC)" for details) and mounted onto gelatinized glass slides (Menzel-Glaser). The slides were dried overnight and coverslipped with Mowiol.

Imaging and Data Analyses

Analyses and photography of fluorescent or DAB stained samples (ICC and immunohistochemistry) were carried out in an inverted Zeiss Axiovert 135 (Oberkochen, Germany) or Leica DM IRB microscope equipped with a digital camera Leica DC100 (Nussloch, Germany). In some experiments, digitized images were captured using Leica IM500 software. Image analyses were performed using NIH Image software. Results are shown as the mean ± S.E. of data from three or four experiments, unless stated otherwise. STATISTICA (StatSoft, Tulsa, OK) software was utilized for all statistical tests. Non-parametric tests were used whenever group variances were different or the data did not fit a normal distribution. ICC, *in vitro* Q-RT-PCR, and behavioral data were analyzed by parametric tests, and *in vivo* Q-RT-PCR was analyzed by a non-parametric test. Also, for FACS experiments, non-parametric tests were used. A significance level of $p < 0.05$ was chosen.

RESULTS

Generation of TH and β-III-tubulin-positive Neurons by Long Term Expanded hVM1 Cells; Effects of Bcl-X$_L$

One of the major hurdles for the generation of stable VM cell lines is the loss of neuron and DAn generation capacity over time (25). Interestingly, the same phenomenon previously observed in neurosphere cultures also occurs in hVM1 cells (Fig. 1, *A–C*). In high passaged cultures, hVM1 cells generated almost no β-III-tubulin$^+$ or TH$^+$ cells (less than 1% of total cells), whereas in low passage cultures, 13.9 ± 0.85 and 10.44 ± 0.81% of the total cells in the cultures were β-III-tubulin$^+$ and TH$^+$, respectively.

Based on previous studies on human forebrain hNSCs (20), we tested the effect of Bcl-X_L in the DAn differentiation potential of hVM1 cells, finding that Bcl-X_L significantly increased the rate of generation of TH$^+$ cells (Fig. 1*D*). Bcl-X_L also induced an increase in β-III-tubulin$^+$ and TH$^+$ cells in a subclone of the hVM1 line (data not shown; subclone 23 in Ref. 15). We therefore generated three stable cell lines from the hVM1 cells by retroviral transduction at low passage (passage 6): hVM1-ø, hVM1-low Bcl-X_L, and hVM1-high Bcl-X_L (Figs. 1*D* and 2*A*). All of the sublines retained multipotency, generating neurons, astroglia, and oligodendrocytes when differentiated *in*

vitro, and have been expanded until passage 36 up to date (over one and a half years in continuous culture). All cell lines used here as well as the parental cells (15) show a normal karyotype with a diploid number of chromosomes ($n = 46$), not showing any numerical or structural chromosomal aberrations by G-banding. The spectral karyotype hybridization analysis confirms the absence of structural rearrangements (see supplemental Fig. S1).

Effects of Bcl-X_L on Cell Death during Cell Differentiation

hVM1 Apoptotic Cell Death during Cellular Differentiation Is Inhibited by Bcl-X_L

When differentiated, control cells (hVM1-ø) but not the Bcl-X_L ones, displayed a massive cell death process (Fig. 2*B*), the mechanism of which was studied analyzing the following apoptotic markers: phosphatidylserine exposure on the outer leaflet of the plasma membrane and DNA fragmentation (Fig. 2, *C* and *D*). Both parameters gradually increased during differentiation of hVM1-ø cells (by day 7, Annexin-V^+ cells were 94.76 ± 1.14% and fragmented DNA was 89.95 ± 0.89% of total cells). Focusing on caspase activation, we found that activated caspase-3 (a general effector caspase) and activated caspase-9 (a mitochondrially activated caspase) were present at much higher levels in differentiated hVM1-ø cells than in Bcl-X_L ones (Fig. 2, *E* and *F*), suggesting a mitochondrial contribution to the cell death process. Mitochondria involvement in the induction/execution process of the apoptotic cell death was confirmed by the nuclear translocation of the apoptotis-inducing factor from the mitochondria to the nucleus at day 3 of differentiation in hVM1-ø cells, otherwise absent in Bcl-X_L cells (supplemental Fig. S2*A*). This event was not caspase-dependent because Z-VAD-fmk had no effect. Mitochondria in control cells lose their inner membrane potential with differentiation, and this depolarization was prevented by Bcl-X_L (supplemental Fig. S3). In summary, hVM1-ø cells die by an apoptotic program involving caspases and mitochondria, and Bcl-X_L (at low or high level) prevents all of these cell death features (Fig. 2, *B–F*, and supplemental Figs. S2*A* and S3).

hVM1 Apoptotic Cell Death Is Reversed by Caspase Inhibition

Cell differentiation was also studied in the presence of the cell death chemical inhibitors *N*-acetylcysteine (NAC; an antioxidant), or Z-VAD-fmk (Fig. 3*A*). NAC treatment did not significantly reduce DNA fragmentation, suggesting that either oxidative stress was not a key factor in cell death or NAC did not inhibit the generation of all types of reactive oxygen species, as proposed previously (26). In contrast, Z-VAD-fmk successfully reduced DNA fragmentation, caspase-3 activation, and phosphatidylserine exposure in the cells (Fig. 3, *A–C*). However, Z-VAD-fmk, by day 7, could not inhibit phosphatidylserine exposure (data not shown) or prevent the nuclear translocation of apoptosis-inducing factor (at day 3) in differentiating hVM1-ø cells (supplemental Fig. S2*A*). Altogether, these data indicated that caspase inhibition successfully revert the cell death but only transiently at early differentiation time points.

DA-derived oxidative stress and DNA damage was previously described to induce DAn death by c-Jun kinase (JNK)

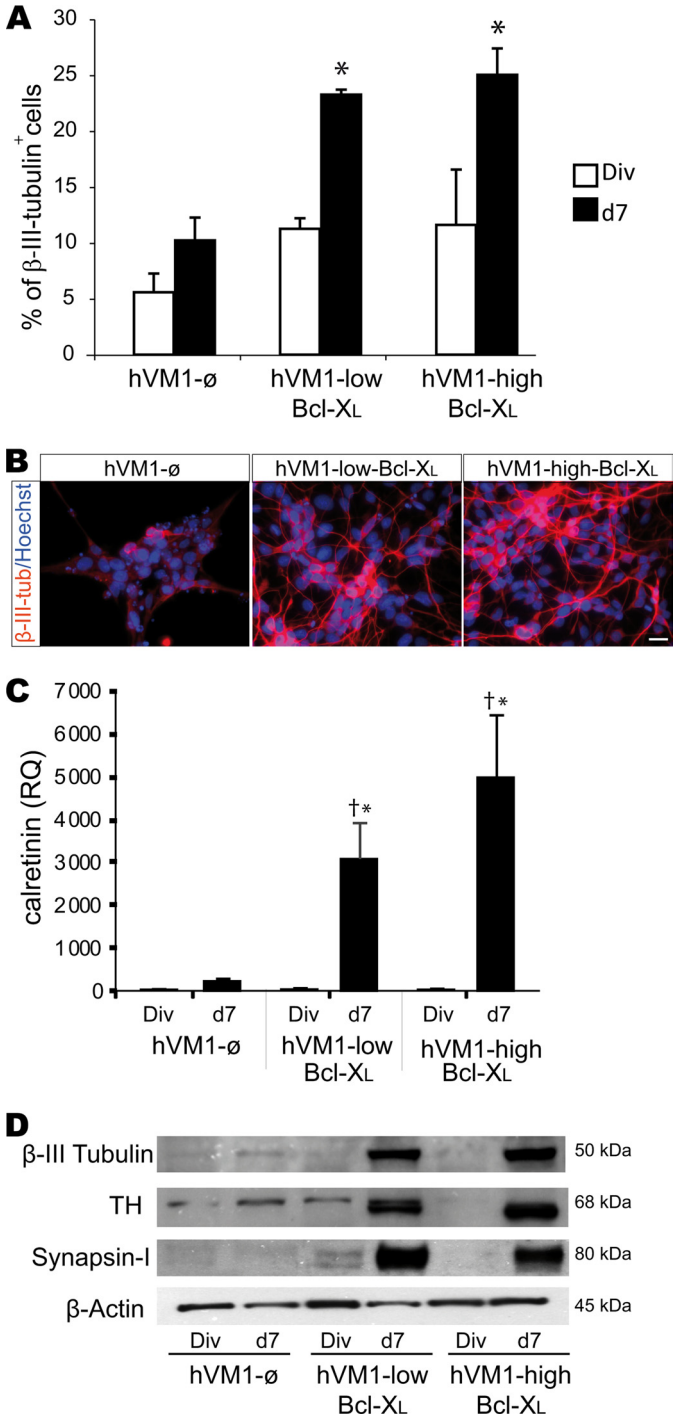

FIGURE 4. **Bcl-X_L effects on neuron and DAn generation by hVM1 cells.** hVM1-ø- or Bcl-X_L-overexpressing cell lines were analyzed under proliferation (*Div*) or after 7 days of differentiation (*d7*). *A*, percentage of β-III-tubulin$^+$ cells was determined by ICC in double-stained β-III-tubulin and Hoechst cultures. Data represent mean ± S.E. ($n = 3$) ($p < 0.05$, Kruskal Wallis ANOVA, post hoc Mann-Whitney *U* test; *, *versus* hVM1-ø cells). *B*, ICC for β-III-tubulin in 7-day differentiated cells. *Scale bar*, 20 μm. *C*, quantitative analysis of *CALRETININ* expression in control and Bcl-X_L-overexpressing cells. Data represent mean ± S.E. ($n = 3$) and were normalized to GAPDH gene expression. RQ is in relation to hVM1-ø cells under division conditions. ($p < 0.05$, ANOVA, post hoc Fisher test; *, *versus* hVM1-ø cells; †, *versus* Div). *D*, Western blots of control, hVM1-low Bcl-X_L, and hVM1-high Bcl-X_L cells under division or differentiation conditions. Blots were stained for β-III-tubulin, TH, synapsin-I, and β-actin.

activation (27). However, JNK inhibition by SP600125 (27, 28), under conditions that block camptothecin-induced apoptosis (not shown), had no effect on cell death of hVM1-ø cells after 3 days of differentiation (supplemental Fig. S2*B*), indicating that JNK does not play a major role in cell death at this stage of differentiation. Furthermore, in an attempt to minimize oxidative stress (29) originating from TH enzyme activity and catecolaminergic metabolism, we used the TH inhibitor α-methyl-*para*-tyrosine (30), but it did not reduce reactive oxygen species in the cultures (H_2O_2 or $O_2^{\cdot-}$, measured with 2′,7′-dicholorodihydrofluorescein diacetate and hydroethidine) or rescued β-III-tubulin- or TH-positive neurons from cell death (results not shown). Altogether, these data suggest that DA-induced oxidative stress does not play a major role in cell death.

Bcl-X$_L$ Protects hVM1 Cells from Cytotoxic Insults

Studies using pharmacologically induced cell death (6-OH-DA, H_2O_2, or camptothecin) indicated that hVM1-ø cells were more sensitive to these agents than Bcl-X_L-overexpressing ones (independently of Bcl-X_L expression level; data not shown). Camptothecin treatment was more toxic (induced a higher DNA fragmentation) than H_2O_2, especially in control cells (Fig. 3*D*). Nevertheless, Bcl-X_L protected hVM1 cells from cytotoxic insults during cellular differentiation (Fig. 3*D*). 6-OH-DA targets DAn when internalized by DAT. In general, we did not observe any toxicity at day 3, suggestive of a lack of DAn maturation.

Effects of Bcl-X$_L$ on Cellular Differentiation

Bcl-X$_L$ Promotes Neuronal and Dopaminergic Differentiation

Bcl-X_L modulates fate decisions of forebrain hNSCs, independently of its antiapoptotic function (19). In the case of hVM1 cells, Bcl-X_L significantly increased (2–2.5-fold)

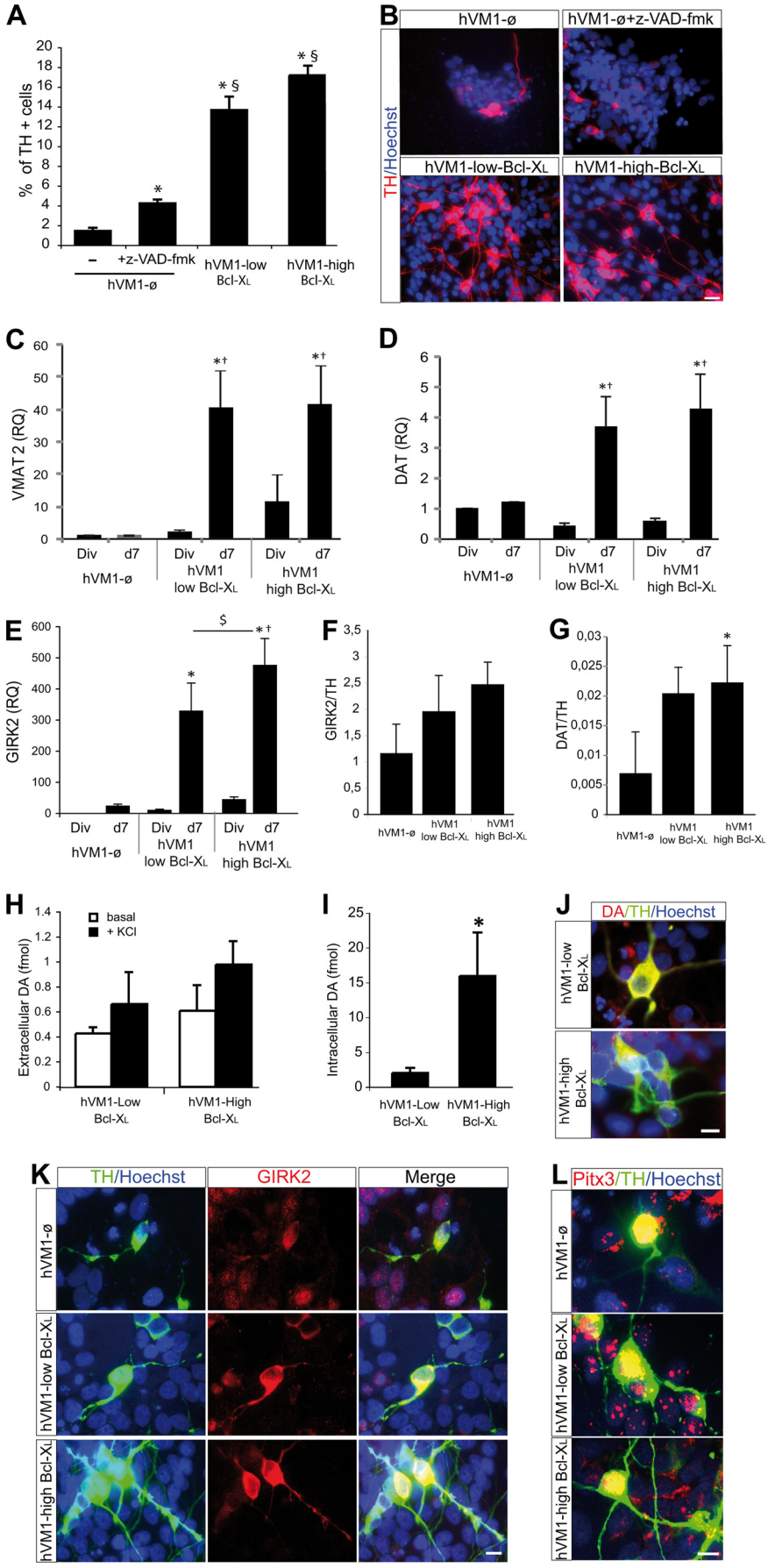

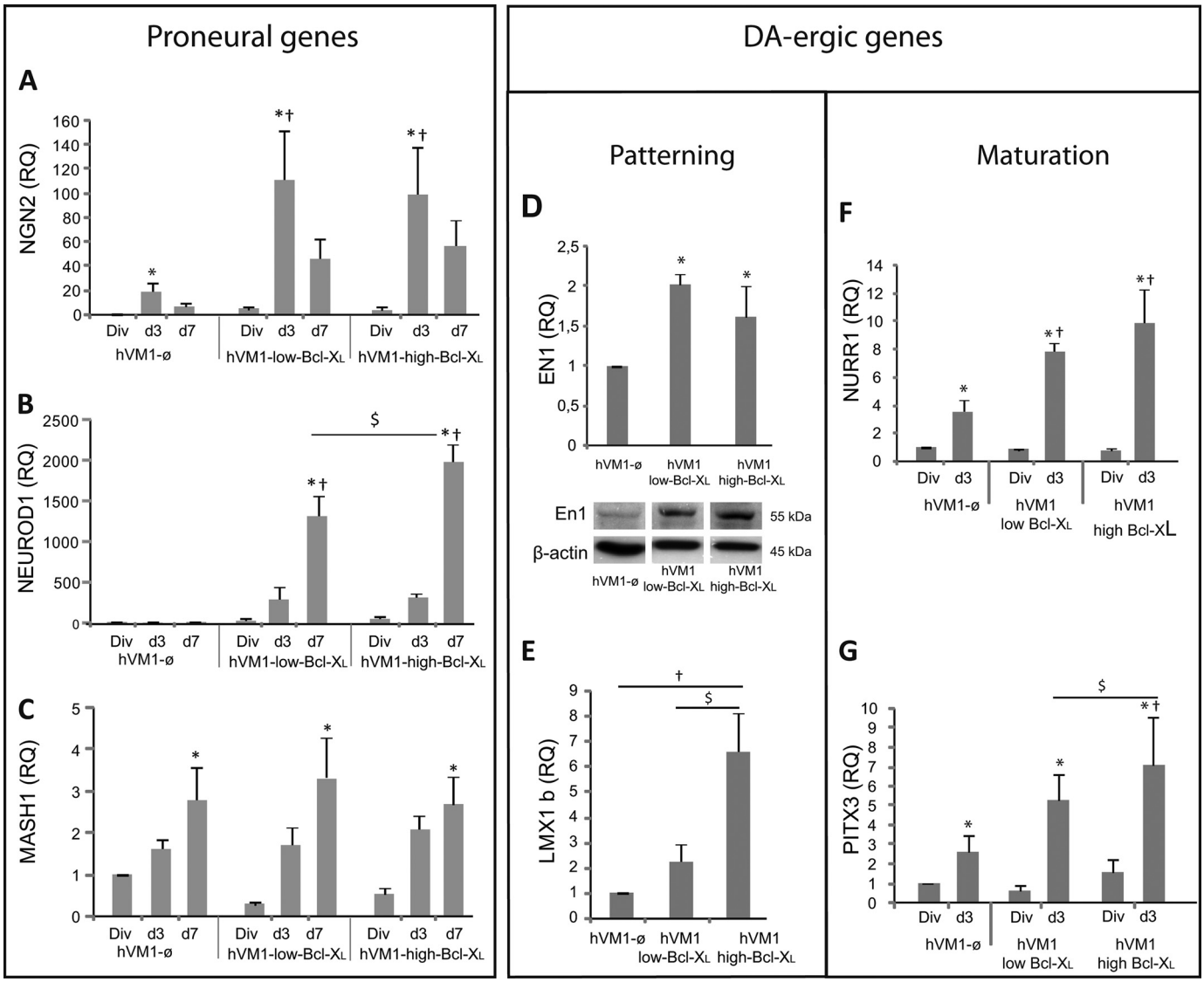

FIGURE 6. **Bcl-X$_L$ effects on proneural and dopaminergic gene expression.** Cell lines were analyzed under division (*Div*) or after 3 and 7 days (*d3* and *d7*) of differentiation. *A–C*, proneural gene expression was determined from division to day 7 of differentiation by analyzing *NGN2* (*A*), *NEUROD1* (*B*), and *MASH1* (*C*). *D* and *E*, expression of genes involved in DAn patterning. *EN1* and *LMX1B* were analyzed in proliferating cells. In relation to *EN1* gene expression, mRNA levels remained elevated in Bcl-X$_L$ overexpressing cells as compared with hVM1-ø cells during the whole differentiation period (not shown). The Western blot shows En1 protein levels in proliferating cells. β-actin was used as loading control. *F* and *G*, expression assay of genes involved in DAn maturation; quantitative expression of *NURR1* and *PITX3* genes in proliferating cells (*Div*) and 3-day (*d3*) or 7-day (*d7*) differentiated cells (results for *VMAT2*, DAT, and *GIRK2* were shown in Fig. 5). *NURR1* and *PITX3* were analyzed and reported in proliferating and in early differentiated cells (*d3*) because these genes were also essential for postmitotic DAn. Data represent mean ± S.E. ($n = 3$ or 5) and were normalized to GAPDH gene expression. RQ was calibrated by referring all data to hVM1-ø cell under division conditions ($p < 0.05$, ANOVA, post hoc Fisher test; *, *versus* Div; †, *versus* hVM1-ø; $, *versus* hVM1-low Bcl-X$_L$).

β-III-tubulin$^+$ cell generation (Fig. 4, *A–D*). Supporting this finding, *CALRETININ* expression (present in mature DAn) (Fig. 4*C*) and synapsin-I levels (involved in synaptic plasticity of functional neurons) were also significantly increased by Bcl-X$_L$ (Fig. 4, *C* and *D*). Concerning dopaminergic differentiation, Bcl-X$_L$ promoted TH$^+$ cell generation after 7 days of differentiation (~10-fold) (Fig. 5, *A* and *B*). Z-VAD-fmk treatment did not change the percentage of β-III-tubulin$^+$ cells (4.66 ± 1.09 and 5.81 ± 0.8%, untreated *versus* Z-VAD-fmk, respectively, $p = 0.15$) and moderately increased TH$^+$ cell number by

FIGURE 5. **Bcl-X$_L$ effects on dopaminergic maturation.** *A*, percentage of TH$^+$ cells after 7 days of differentiation of control or Bcl-X$_L$-overexpressing hVM1 cells. hVM1-ø cells were treated with 50 μM Z-VAD-fmk ($p < 0.05$, Kruskal Wallis ANOVA, post hoc Mann-Whitney *U* test; *, *versus* hVM-ø cells; $, *versus* hVM1-ø + Z-VAD-fmk). *B*, pictures illustrate ICC staining for TH and Hoechst. *Scale bar*, 20 μm. *C–E*, Q-RT-PCR for *VMAT2*, DAT, and *GIRK2* in dividing and 7-day differentiated control or Bcl-X$_L$-overexpressing cells. Data represent mean ± S.E. ($n = 3$) and were normalized to GAPDH gene expression. RQs were referred to hVM1-ø cells under division conditions ($p < 0.05$, ANOVA, post hoc Fisher test; *, *versus* hVM1-ø cells; †, *versus* Div; $, *versus* hVM1-low Bcl-X$_L$). *F* and *G*, *GIRK2* and DAT Q-RT-PCR data from 7-day differentiated cells were relative to TH expression levels, respectively ($n = 3$, $p < 0.05$, ANOVA, post hoc Fisher test; *, *versus* hVM1-ø cells). *H* and *I*, DA detection by HPLC in 7-day differentiated Bcl-X$_L$-overexpressing cell lines. The *histograms* represent intracellular DA content and released DA (in basal or KCl-induced depolarization conditions) ($n = 3$; *, $p < 0.05$, Mann-Whitney *U* test). DA could not be reliably detected in control cells, possibly due to the high rate of cell death by day 7 of differentiation. *J*, DA/TH double ICC in 7-day differentiated hVM1-low Bcl-X$_L$ and hVM1-high Bcl-X$_L$ cells. *Scale bar*, 10 μm. *K* and *L*, double ICC for TH and GIRK2 and TH and Pitx3 in 7-day differentiated cells (*scale bar*, 10 μm).

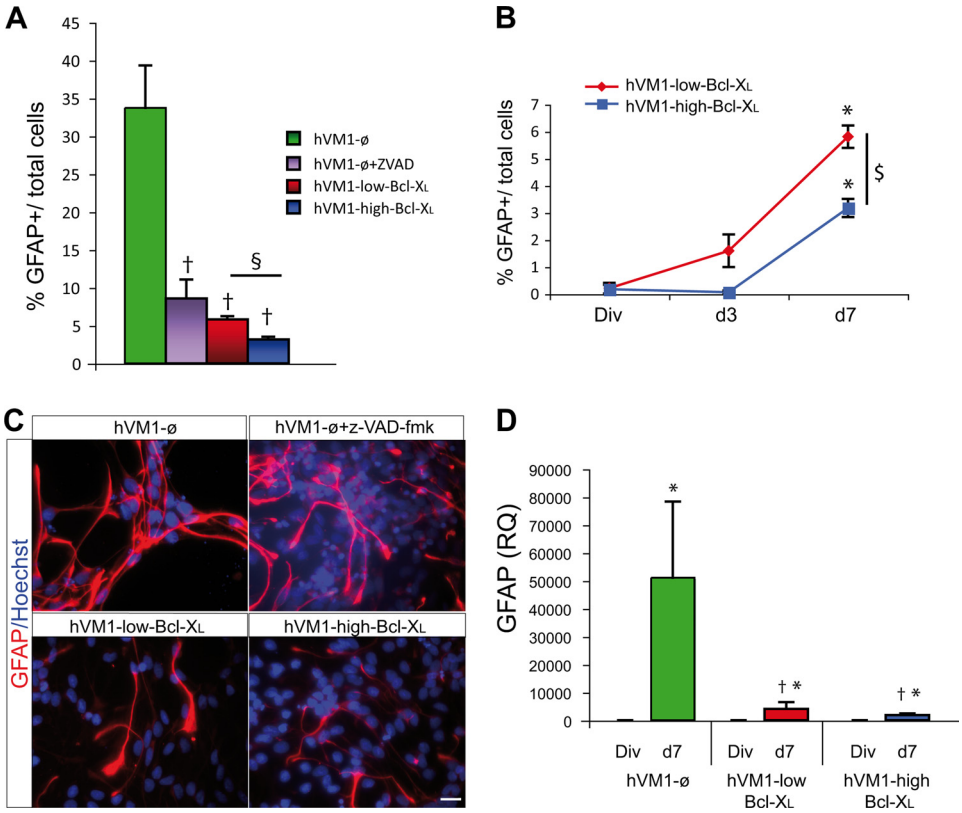

FIGURE 7. **Bcl-X$_L$ effects on glial differentiation.** *A*, percentage of GFAP$^+$ cells after 7 days of differentiation of hVM1-ø cells treated or not with 50 μM Z-VAD-fmk, hVM1-low Bcl-X$_L$, and hVM1-high Bcl-X$_L$. *B*, percentage of GFAP$^+$ cells in dividing cells and after 3 and 7 days of differentiation in both overexpressing Bcl-X$_L$ cell lines. Data represent mean ± S.E. ($n = 3$) ($p < 0.05$, Kruskal Wallis ANOVA, post hoc Mann-Whitney *U* test; *, *versus* Div; †, *versus* hVM1-ø; $, *versus* hVM1-low Bcl-X$_L$). *C*, ICC for GFAP. Nuclei were counterstained with Hoechst. *Scale bar*, 20 μm. *D*, GFAP gene expression. Data represent mean ± S.E. ($n = 3$). ($p < 0.05$, ANOVA, post hoc Fisher test; *, *versus* Div; †, *versus* hVM1-ø).

hVM1-ø cells, but TH$^+$ cells did not reach the levels generated by Bcl-X$_L$ ones (Fig. 5*A*). Bcl-X$_L$ also induced a significant increase in the expression of the DAn-related genes *VMAT2*, DAT, and *GIRK2* (Fig. 5, *C–E*). In the case of *GIRK2*, Bcl-X$_L$ exerted a dose-dependent effect (Fig. 5*E*). The ratio of gene expression *GIRK2*/TH and DAT/TH (both indicating maturation of TH$^+$ cells) increased in Bcl-X$_L$ cells as compared with control ones (Fig. 5, *F* and *G*). Moreover, DA synthesis was dramatically increased by Bcl-X$_L$ (Fig. 5*I*).

TH$^+$ cells did not co-stain with GABA, glutamate, or serotonin (supplemental Fig. S4), and dopamine β-hydroxylase mRNA, needed to progress into the adrenergic pathway, was not detected in hVM1 cells or derivatives by Q-RT-PCR (data not shown). The genuine SNpc nature of TH$^+$ neurons was further demonstrated by the expression of *VMAT2*, DAT, and *GIRK2* genes (Fig. 5, *C–E*) and by the co-localization of TH/Girk2 and TH/Pitx3 proteins in differentiated cells (independently of Bcl-X$_L$ levels) (Fig. 5, *K* and *L*).

Developmental Genes

Proneural—NGN2 is essential for cell cycle exit and neuronal differentiation of NSCs and for DAn generation (31). As expected for an early proneural gene, *NGN2* expression peaked at 3 days of differentiation and was enhanced by Bcl-X$_L$, decreasing later (day 7), when neurons become postmitotic (32) (Fig. 6*A*). Consistently, hVM1 cells displayed a postmitotic profile after 3 days of differentiation (supplemental Fig. S5). *NEUROD1* (a target of Ngn2) expression steadily increased with differentiation time (Fig. 6*B*), and Bcl-X$_L$ induced a dramatic dose-dependent increase in its expression level. On the contrary, Bcl-X$_L$ did not affect *MASH1* expression during differentiation (Fig. 6*C*).

Dopaminergic—EN-1 and *LMX1B* (involved in DAn patterning, specification, and survival) expression was enhanced by Bcl-X$_L$, in a dose-dependent manner in the case of *LMX1B* in proliferating cells (Fig. 6, *D* and *E*). Differentiation triggered the expression of *NURR1* (involved in patterning and cell cycle exit of SNpc DAn precursors) and *PITX3* (involved in DAn induction/differentiation and closely related to *LMX1B* expression (33)) (Fig. 6, *F* and *G*), and again, Bcl-X$_L$ further enhanced them, consistent with a correct patterning of the precursors, induction of cell cycle exit, and increased SNpc DAn generation rate (Fig. 5). In parallel to *LMX1B*, Bcl-X$_L$ promoted *PITX3* expression in a dose-dependent manner because both share a common pathway for DA-ergic induction (33) (Fig. 5, *E* and *G*). Because being postmitotic is a *sine qua non* condition for the induction and maturation of DAn, cell cycle exit (measured by flow cytometry) paralleled the increased expression of NURR1 and PITX3 (supplemental Fig. S5, *A–C*).

In summary, these data provide evidence for a novel action of Bcl-X$_L$ inducing neuronal and dopaminergic differentiation by promoting the expression of proneural (*NGN2* and *NEUROD1*) and DA patterning-, differentiation-, and maturation-related genes (*EN1*, *LMX1B*, *PITX3*, *NURR1*, *VMAT2*, and DAT).

Bcl-X$_L$ Reduced Glial Cell Generation—Finally, Bcl-X$_L$ induced a dose-dependent significant decrease in GFAP$^+$ cells (Fig. 7, *A–C*). In Z-VAD-fmk-treated hVM1-ø cells, GFAP$^+$ cells significantly decreased when compared with untreated hVM1-ø cells but remained higher than in Bcl-X$_L$ cells (Fig. 7*A*). ICC studies were confirmed by Western blot (not shown) and Q-RT-PCR assays, both confirming that Bcl-X$_L$ decreases glial cell generation (Fig. 7*D*).

Transplantation of hVM1 Cell PD Rat Models; Effects of Bcl-X$_L$

hVM1-ø and hVM1-high Bcl-X$_L$ cells were studied *in vivo* in hemiparkinsonian rats (Fig. 8*A*). The hVM1-low Bcl-X$_L$ cell line was not included because it had lower DA content and generated fewer DAn *in vitro*.

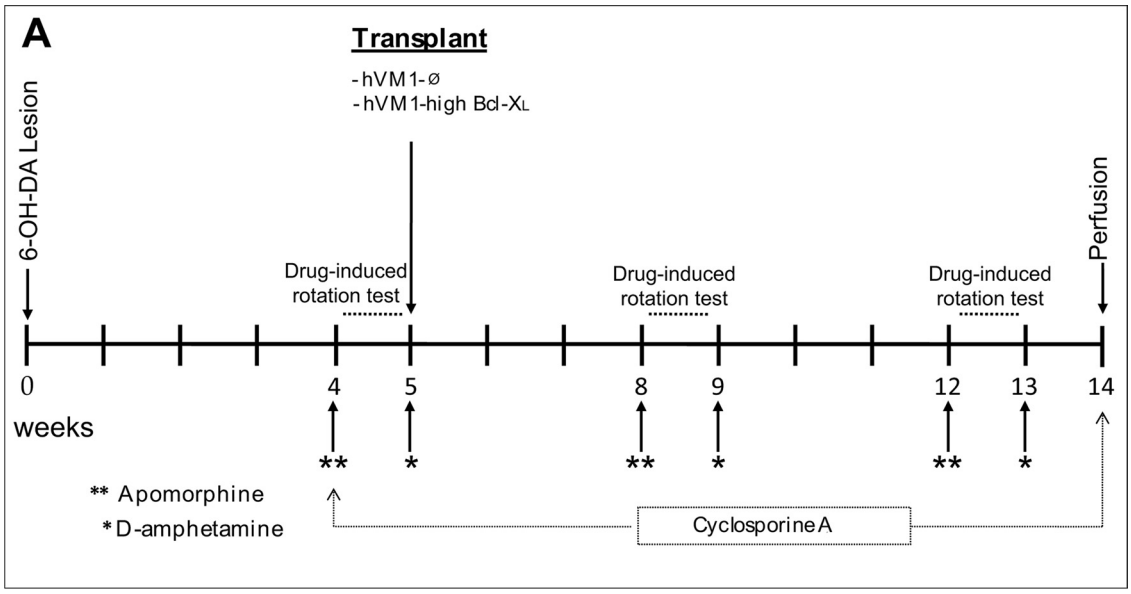
A
Transplant
- hVM1-ø
- hVM1-high Bcl-XL
6-OH-DA Lesion
Drug-induced rotation test
Drug-induced rotation test
Drug-induced rotation test
Perfusion
0
4
5
8
9
12
13
14
weeks
**
*
**
*
**
*
** Apomorphine
* D-amphetamine
Cyclosporine A

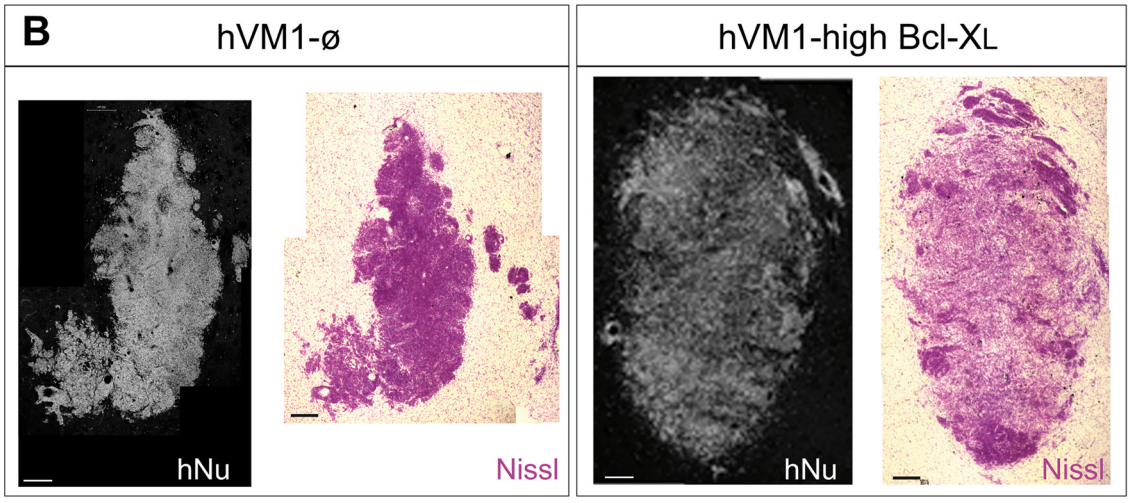
B
hVM1-ø
hVM1-high Bcl-XL
hNu
Nissl
hNu
Nissl

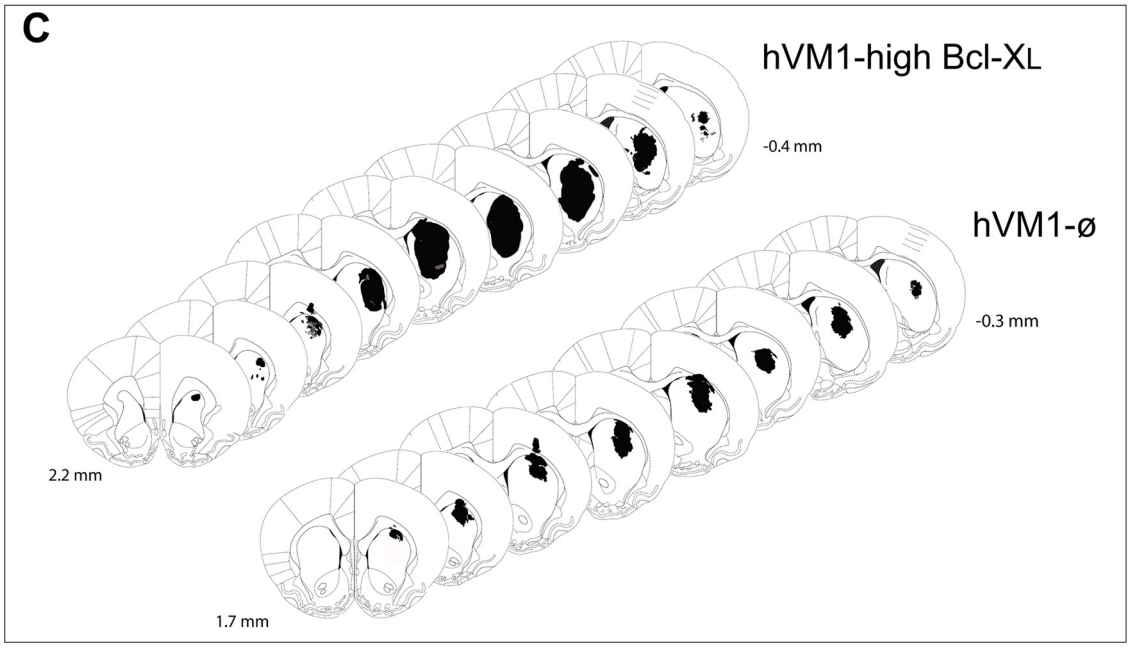
C
hVM1-high Bcl-XL
-0.4 mm
hVM1-ø
-0.3 mm
2.2 mm
1.7 mm

At 2 months post-transplantation, both cell types survived and integrated well into the host parenchyma (hNu and Nissl stainings; Fig. 8*B*), not generating tumors. Macroscopically, the grafts formed a morphologically compact group in the host striatum (Fig. 8, *B* and *C*). Only a few migrating cells (Dcx$^+$/hNu$^+$) were detected around the grafts (Figs. 8*B* and 9, *A* and *B*), in contrast to the extensive migratory capacity of forebrain hNS1 cells (human immortalized neural stem cell line derived from fetal forebrain) previously described (34). Bcl-X$_L$ cell grafts were larger than hVM1-ø cell grafts (1.52 $\pm$ 0.55 mm^3 *versus* 0.19 $\pm$ 0.09 mm^3) and colonized more extensive striatal regions (Fig. 8*C*), suggesting a healthier state than the control ones and supporting *in vitro* data (Figs. 2 and 3).

At the cellular level, stereology could not be performed accurately because the morphology, density, and three-dimensional arrangement of the cells precluded in many cases the identification of individual cells in the randomized microscopic fields. In any case, microscopic examination of the grafts revealed strongly stained GFAP$^+$ cells in both animal groups (Fig. 9, *C* and *D*). Qualitative assessment was suggestive of a lower number of GFAP$^+$ cells in the hVM1-high Bcl-X$_L$ grafts when compared with the control ones. Strong staining for neuronal markers was also observed, such as for immature migrating neuroblasts (Dcx$^+$/hNu$^+$ cells) (Fig. 9, *A* and *B*) and mature neurons (hNSE$^+$ cells) (Fig. 9, *I* and J). In relation to DA-ergic differentiation, TH$^+$/hNu$^+$ and TH$^+$/hNSE$^+$ cells were present in both transplant types (Fig. 9, *E–J*). TH staining was heterogeneous within a graft, with regions rich in TH$^+$ cells interspersed with areas devoid of them. Qualitatively, TH$^+$ cells were more abundant in the hVM1-high Bcl-X$_L$ group (Fig. 9, *E* and *F*). At 2 months post-transplantation, TH$^+$ cells were also positive for the mature neuronal marker hNSE (Fig. 9, *I* and *J*), and occasionally, we could detect the presence of human TH$^+$/DAT$^+$/rhGFP$^+$ cells (not shown), indicating the acquisition of a mature neuronal and DA-ergic phenotype *in vivo* of the transplanted cells.

In order to analyze graft development/maturation and quantify Bcl-X$_L$ effects, an independent set of animals was transplanted and behaviorally tested, but their brains were used for gene expression studies (Q-RT-PCR; Fig. 10, *A–E*). There was more mRNA for β-III-tubulin and TH in absolute terms (as compared with 18 S; Fig. 10, *A* and *B*). When the TH mRNA level was normalized to that of β-III-tubulin (*i.e.* indicating, among neurons, how many were TH), we found that more TH mRNA was present in Bcl-X$_L$ grafts (Fig. 10*C*). In relation to DA maturation, abundant mRNA for DAT and GIRK2 was detected in both transplant types; in absolute terms (the data relative to 18 S), Bcl-X$_L$ induced a 2–3-fold increase in DAT and GIRK2, as shown in Fig. 10, *D* and *E* (non-significant difference, $p = 0.08$ and $p = 0.2$, respectively, Mann-Whitney *U* test).

Rotational behavior was studied in both sets of animals (those destined for histology and the gene expression animals; total $n = 12$ for control, $n = 13$ for Bcl-X$_L$) (Fig. 10, *F* and *G*). Apomorphine-induced rotation was not compensated, neither in control nor in Bcl-X$_L$ animals (Fig. 10*F*). In contrast, in the case of amphetamine-induced rotation, although there were no signs of recovery in the control cell-grafted animals, the ones receiving Bcl-X$_L$ transplants significantly improved (Fig. 10*G*). These results are substantiated by the findings in the histology and Q-RT-PCR studies (namely that there are DAn in the transplants mature enough to produce and release DA after drug stimulation and that their maturation or functional integration into the circuitry of the host striatum is enhanced by Bcl-X$_L$ but still limited at 2 months postgrafting).

DISCUSSION

Presently, fresh fetal VM tissue constitutes the best choice to obtain large numbers of human genuine and functional SNpc DAn for cell replacement therapy for PD (5, 35). Human VM cell cultures present limited proliferation and usually fail to maintain their DAn generation potential when cultured long term (36). In the present report, we described this last phenomenon in a new immortalized hVM1 stem cell line (15), meaning that genetic perpetuation of VM cells, while allowing for long term proliferation, is not sufficient to preserve differentiation properties (in contrast to the stability conferred to forebrain hNSCs) (37). In this scenario of declining neurogenic and DA-ergic potential, we asked whether Bcl-X$_L$ could preserve the DAn generation capacity of hVM1 neural stem cells, and our findings consistently demonstrate that it can. On the one hand, Bcl-X$_L$ protects from the massive natural apoptotic cell death occurring during cellular differentiation and after a cytotoxic insult. In addition, we have found a novel action of Bcl-X$_L$ in VM cells, that of modulating cellular differentiation through the activation of specific sets of transcription factors, increasing neuronal and dopaminergic differentiation in a dose-dependent way while inhibiting glial cell generation. Furthermore, *in vivo* studies demonstrated that hVM1-derived cell lines survived and integrated into the hemiparkinsonian brain, generating neurons and DAn, which where more abundant when Bcl-X$_L$ levels were augmented. Bcl-X$_L$ enhanced the *in vivo* functional recovery induced by hVM1 cell grafts, which can be explained by a combined enhancement of survival and differentiation of the transplanted cells.

Bcl-X$_L$ Protects from Cell Death—Bcl-X$_L$ is an antiapoptotic protein, key for central nervous system development and neuron (38) and DAn survival (17, 21, 39). We demonstrate here that Bcl-X$_L$ protected hVM1 NSCs from apoptosis during differentiation and in response to cytotoxic insults. Apoptotic cell death in differentiating hVM1-ø cells was generalized (not DAn-specific) and started at early differentiation time points (such as in mouse and human embryonic stem cells and throughout brain development) (21, 40, 41). Mechanistic stud-

FIGURE 8. **Transplantation of hVM1-ø and hVM1-high Bcl-X$_L$ cells in a rat model of PD.** *A*, time course of surgery and drug rotation tests. Rats received a complete 6-OHDA lesion of the right nigrostriatal system (median forebrain bundle; *MFB*) prior to cellular transplantation in the lesioned striatum. Changes in rotation behavior were assessed in three sessions, one postlesion and two postgrafting, as indicated. The animals were immune suppressed with daily intraperitoneal injections of cyclosporin A during the whole experiment. *B*, photomicrographs of coronal sections from striatum showing representative transplants stained for human nuclei and Nissl (*scale bar*, 200 μm). *C*, rostrocaudal series bearing the transplants from representative animals. Note that the Bcl-X$_L$ graft spans larger regions in all three axes (anteroposterior, mediolateral, and dorsoventral). Paxinos coordinates for the first and last section containing the graft are given.

ies revealed that caspase activation and mitochondria (by the release of apoptosis-inducing factor, caspase-9 activation, and loss of $\Delta\Psi_{mit}$) were directly involved in this process. Caspases inhibition delayed but not abolished cell death pointing to the involvement of a caspase-independent way, as it was previously described in neuronal populations (42).

Bcl-X_L was more potent at preventing cell death than chemical agents, like anti-oxidant (NAC), TH inhibitor (α-methyl-*para*-tyrosine), JNK, or caspase inhibitors. This may be explained by the fact that Bcl-X_L directly inhibits the initiation of the cell death program at several points (loss of $\Delta\Psi_{mit}$ and mitochondrial permeabilization, resulting in reduced caspase activation and DNA fragmentation), thus providing enough survival signals to allow the cells to engage and progress through the differentiation process.

Bcl-X_L Modulates Cell Fate, Promoting the Neuronal and Dopaminergic Phenotype—To our knowledge, other reported human fetal VM cell strains/lines did only generate genuine SNpc DAn at low passage number in culture (until passage 10) (43, 44). Therefore, the problem of obtaining a continuous, reliable source of transplantable SNpc DAn remained. In the present study, we demonstrate one way to overcome this limitation, using Bcl-X_L, which turns VM hNSCs in a stable source of genuine SNpc DAn.

Recent studies described that Bcl-X_L was directly involved in the modulation of central nervous system development, hematopoietic progenitor cell differentiation, and embryonic stem cells (19, 21, 45, 46). Bcl-2 and Bax (Bcl-2-associated X protein) were also shown to induce the commitment of progenitor cells (41, 47). Because the main research focus around the Bcl-2 family of proteins is related to apoptosis regulation, other mechanisms by which these proteins could modulate cellular commitment and differentiation have remained elusive and controversial but are becoming steady and firmly established (19, 45, 48, 49). A conservative view would be that of Boeuf *et al.* (41, 50, 51), who underlined that the cell commitment modulation exerted by Bcl-2 proteins was closely related to their survival function, through the regulation of the mitogen-activated protein kinase pathway. In our model, Bcl-X_L displayed an important antiapoptotic role in differentiating cells, but this is insufficient to explain the observed effects and needs to be considered in combination with the induction of neurogenesis (see the model in Fig. 11). For instance, cell death inhibition (by Z-VAD-fmk) only results in an increase of 2–3-fold in TH^+ neurons, as compared with the 10-fold enhancement occurring after increasing Bcl-X_L levels (Fig. 5*A*). Because a mechanistic explanation for the induction of neurogenesis by Bcl-X_L was lacking, after clarifying its role and mechanism counteracting cell death, we focused on proneural and DA-ergic (patterning and maturation) gene expression.

In the present study, we demonstrate a novel function of Bcl-X_L in hNSCs and VM in particular, that of enhancing the expression of proneural genes (*NGN2* and *NEUROD1* but not *MASH1*), *NEUROD1* being induced in a dose-dependent manner. This mechanism explains neuronal induction independently of an antiapoptotic action. Furthermore, although differences in neurogenesis were noted between the two Bcl-X_L cell lines used here, no differences in cell death rate were observed. In addition, cells from Clone 23 (a subclone of the control hVM1 cell line that was later modified to overexpress Bcl-X_L) do not undergo any cell death, and in these cells too, Bcl-X_L results in the generation of more neurons and DAn.[3] Therefore, cell death counteraction as the sole mechanism operating is clearly insufficient to explain Bcl-X_L actions on VM cells.

In other model systems, Bcl-X_L has also been shown to induce neurogenesis independently of its action counteracting cell death. Thus, in forebrain hNSCs, which do not undergo substantial cell death during differentiation, Bcl-X_L enhances neuron generation 3-fold and TH^+ neuron generation 100-fold (19, 20). In forebrain hNSCs too, the Bcl-X_L Y101K mutant lacking the cell survival function (Bax binding domain deleted) (46) shows the same potency for neurogenesis enhancement as the wild type.[4] Last, similar Bcl-X_L effects on neurogenesis have been described in rats and mice (45).

Turning to effects on DA-ergic developmental genes, Bcl-X_L shows a dose-dependent effect on *LMX1B* expression, indicating that, well before the cell death process is initiated (day 3), Bcl-X_L modulates the expression of dopaminergic patterning factors. *PITX3*, a direct target of *LMX1B*, was logically induced in the same manner (see model in Fig. 11). Thus, TH expression and then DAn generation is enhanced by Bcl-X_L, depending on its expression levels (33, 52, 53). In addition, Bcl-X_L also enhances other molecular pathways involved in DAn generation by inducing earlier transcription factors, such as En1, in mitotic precursors. Nurr1 and TH were subsequently induced during differentiation, as the cells progressed to a postmitotic stage (note that Ngn2 and Nurr1 actions are essential for correct and full maturation to DAn (31, 54)). It is interesting to emphasize that En1, in addition to its patterning effect, acts as a survival factor for VM DAn, thus implying that Bcl-X_L effect on DAn induction may be complemented by DAn survival promotion (55).

All of these Bcl-X_L effects were specific to VM cells because Bcl-X_L induced TH expression but not *LMX1B*, *EN1*, *NURR1*, or *PITX3* expression in forebrain hNSCs.[5] This is consistent with the view that human fetal VM hNSCs were already adequately patterned *in vivo* at the time of tissue procurement to express SNpc DAn-specific transcription factors, when compared with non-VM tissue (6).

Thus, we propose a model where TH induction (as well as *VMAT2*, DAT, and *GIRK2* increased gene expression) and the consequent increased DAn production are explained by the Bcl-X_L effect on patterning factors involved in dopaminergic differentiation (part of these increases being directly dependent on the Bcl-X_L dose). What remains to be elucidated and constitutes the focus of ongoing and future studies is the precise molecular event by which Bcl-X_L controls gene expression, if it is a direct or indirect action on chromatin or the result of an enhanced cellular health status, and the mediators playing a role in this last case.

In summary, Bcl-X_L enhances the net yield of neurons and DAn by several mechanisms operating in a synergistic manner:

[3] E. T. Courtois, unpublished results.
[4] E. García-García and A. Martínez-Serrano, unpublished results.
[5] E. G. Seiz, unpublished results.

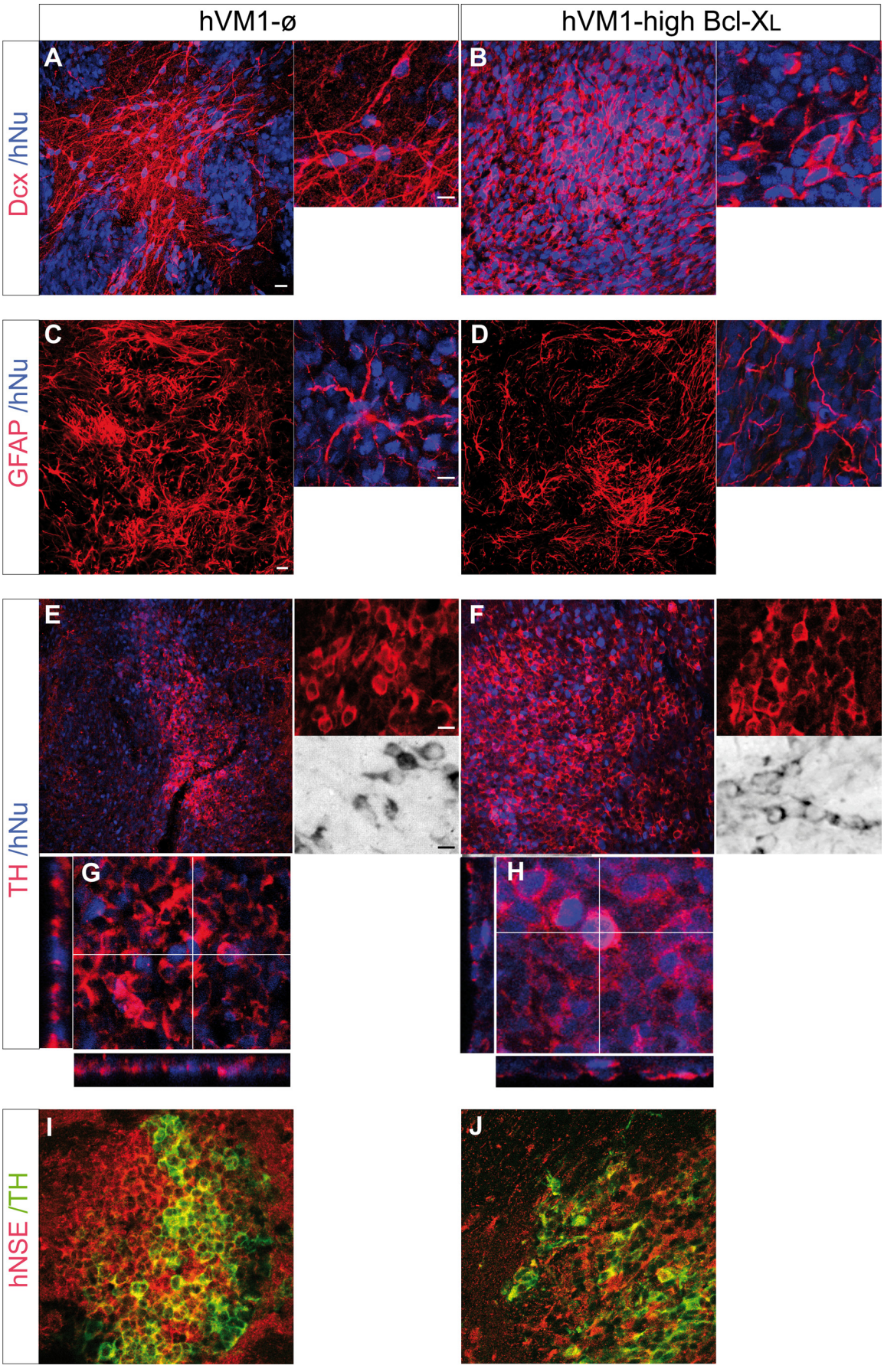
hVM1-ø
hVM1-high Bcl-XL
Dcx /hNu
GFAP /hNu
TH /hNu
hNSE /TH
A
B
C
D
E
F
G
H
I
J

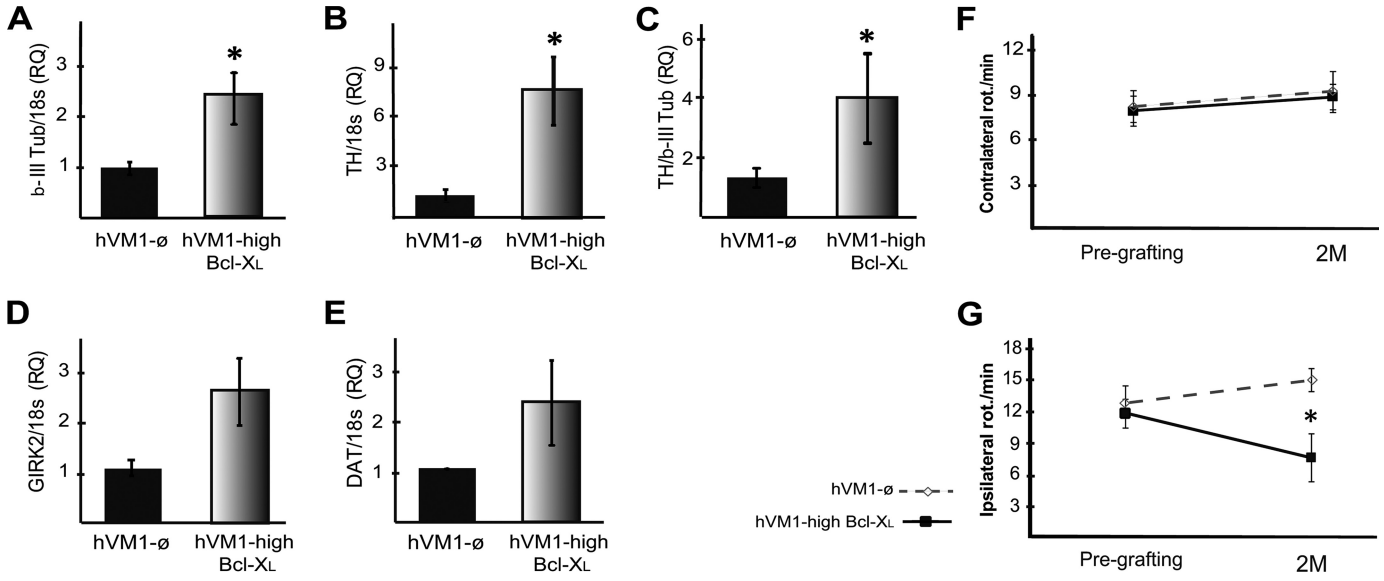

FIGURE 10. **Q-RT-PCR *in vivo* of human genes and behavioral results.** *A–E*, gene expression. Rats were transplanted as described under "Experimental Procedures." After 2 months, brains were processed for RNA extraction and Q-RT-PCR detection of β-III tubulin (neurons) (*A*), DAn (TH) (*B*), SNpc origin (GIRK2) (*D*), and maturation (DAT) of DAn (*E*). Data show higher levels of neuronal, dopaminergic, and SNpc genes in hVM1-Bcl-X$_L$ grafts compared with control grafts (hVM1-ø), suggestive of more neurons and mature DA neurons ($n = 5$ and 6, respectively, mean ± S.E.; *, $p < 0.05$, Mann-Whitney *U* test). *C*, the ratio TH/β-III-tubulin represents the dopaminergic field of the generated neurons after 2 months of transplantation. Determination of gene expression was made with human-specific probes, not cross-reacting with rat genes. RNA integrity was confirmed by 18 S rRNA expression. RQ was calibrated by referring all data to the hVM1-ø cells transplanted group. *F* and *G*, behavioral results. *F*, contralateral apomorphine-induced rotation (for hVM1-ø and hVM1-high Bcl-X$_L$ groups, $n = 12$ and 11, respectively). *G*, intrastriatal grafts of hVM1-high Bcl-X$_L$ cells induce partial compensation of the lesion-induced rotational asymmetry in the D-amphetamine-induced rotation test (for hVM1-ø and hVM1-high Bcl-X$_L$ groups $n = 13$ and 9, respectively). In both cases, data are expressed as turns/min. Rotation tests were run at pregrafting (*PG*) and 2 months post-transplantation (*2M*). Data represent mean ± S.E. Data were analyzed by two-way ANOVA, with least square difference post hoc test (*, $p < 0.05$ *versus* hVM1-ø).

first by counteracting cell death, second by inducing proneural genes, and third by promoting the specification, maturation, and survival of the DAn generated through the induction of a set of strictly DA-ergic transcription factors.

Bcl-X$_L$ also inhibited GFAP$^+$ cell generation, which can be explained by the increased *NGN2* expression, because neurogenin can repress GFAP gene expression (56). In our system, Bcl-X$_L$ decreased glial (GFAP$^+$) cell generation in a dose-dependent manner, but no dose effect was seen in *NGN2* expression, indicating that an alternative or additional pathway must be implicated in the antigliogenic Bcl-X$_L$ action. The glia-neuron shift observed in hVM1 cells could be due to a reduced caspase-3 activation, which would be consistent with the reports indicating that caspase proteins may induce neurogenesis and inhibit glial cell generation (57, 58). However, GFAP data suggested again that the Bcl-X$_L$ effect on cellular commitment was different from its antiapoptotic function because no differences between hVM1-low Bcl-X$_L$ and hVM1-high Bcl-X$_L$ cell death rate were observed, whereas glia generation was different.

Bcl-X$_L$ Promotes Functional Recovery in Hemiparkinson Rat Models—Only one of the reported human fetal VM NSC lines (8, 14, 59), MESC2.10, has been transplanted (10). These cells were described to be phenotypically unstable, and no TH$^+$ cells were observed in the transplants. In the present study, hVM1-derived cell lines did survive and integrate well at 2 months after transplantation. hVM1 grafts generated mature neurons (and glial cells) in the adult striatum, a typically non-neurogenic environment. Many TH$^+$ cells and also some mature DAn (TH$^+$/DAT$^+$) were detected in hVM1 control cell transplants, meaning that the immortalized VM cell line maintains its potency to generate DAn *in vivo*. Q-RT-PCR *in vivo* data confirmed this fact. Furthermore, it provided quantitative evidence allowing us to state that in Bcl-X$_L$ transplants, there were more dopaminergic neurons and that these tended to be more mature than in the control grafts. Collectively, these histological, cellular, and molecular data explain why Bcl-X$_L$ transplants enhanced behavioral recovery, otherwise absent in control cell transplanted animals. The observed behavioral effect must be due to vesicular dopamine release from the TH$^+$, DA-ergic neurons present. However, their degree of maturation seems to be incomplete (although enhanced to some extent by Bcl-X$_L$) because compensation of apomorphine-induced rotation, which requires normalization of DA receptor expression in target striatal GABA-ergic neurons, did not occur. Behavioral recovery was not complete at the time point studied (2 months), consistent with the well known fact that even fresh fetal tissue requires longer periods (3–6 months) *in vivo* to generate fully functional DAn (60). Therefore, future studies will be focused on determining the therapeutic effect of hVM1 cells at longer time points (up to 12 months) and on elucidating whether improved maturation occurs over sev-

FIGURE 9. **Cellular analyses of the transplants.** Transplants were stained for Dcx (*A* and *B*), human GFAP (*C* and *D*), TH (*E–H*), and hNSE (*I* and *J*) (and counterstained with hNu). For each staining, both low magnification (*left*) and a high power image (*right*) are shown. For TH immunohistochemistry, DAB-stained cells are shown in *E* and *F*, and orthogonal projections are shown, confirming the colocalization of TH and hNu (*G* and *H*). *Scale bars* in low magnification images, 20 μm; *scale bar* in the high power image, 10 μm.

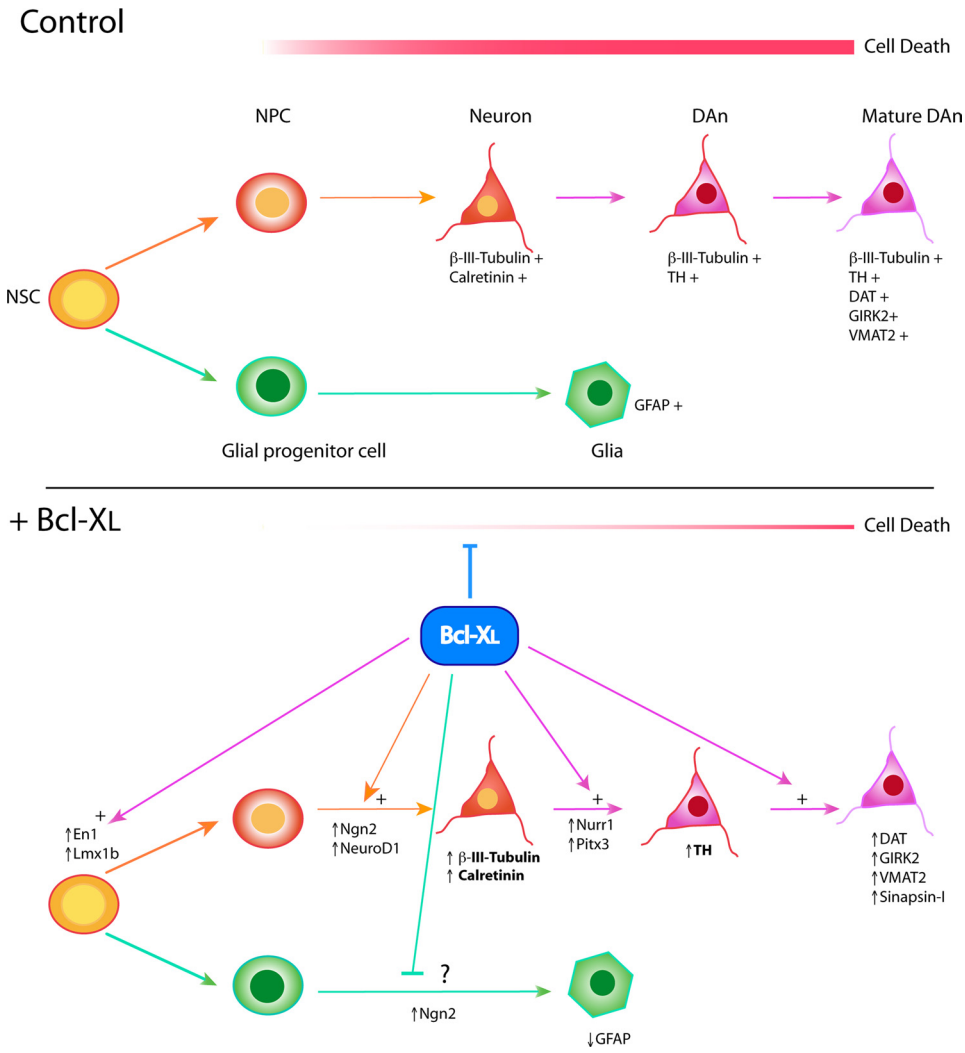

FIGURE 11. **Proposed model of Bcl-X$_L$ effects on human VM NSC differentiation.** In a control situation, hVM1-ø cells first differentiate to neuronal (NPC) and glial progenitors and then generate neurons (*β*-III-tubulin$^+$) and glial cells (GFAP$^+$). Additional signals are required to generate DAn (TH$^+$) and mature DAn (also expressing markers like VMAT-2, DAT, and GIRK2). Cell death occurs during the whole of the differentiation process. Bcl-X$_L$ exerts three actions. First, it counteracts cell death (at multiple levels). Second, Bcl-X$_L$ promotes neuron generation by inducing proneural factors (Ngn2 and NeuroD1) at early times during differentiation. Third, Bcl-X$_L$ potentiates dopaminergic differentiation, first enhancing DA-ergic patterning factors (Lm1xb, En1, Nurr1, and Pitx3) and later inducing factors involved in maturation of the DAn (GIRK2, VMAT2, and DAT). Phenotypic markers in *boldface type* are increased in a Bcl-X$_L$ dose-dependent way.

eral months. In previous studies, we demonstrated that Bcl-X$_L$ did improve DAn generation *in vivo* from forebrain NSCs (20), but those transplants did not induce any behavioral recovery.[6] This suggests that the behavioral effect described in this report must be due to the VM origin of the cells and to the increased DAn generation and concomitant DA release in the host brain. Striatal DA levels, requiring additional animals, were not measured in the present proof of principle experiment because, due to the short survival time, statistically significant differences between control and Bcl-X$_L$ cell-grafted animals were not expected. Last and as it happens also for human embryonic stem cells (21), it is important to be aware that, since Bcl-2 is a well known proto-oncogene, detailed, long term studies should be conducted to establish if Bcl-X$_L$ overexpression results in tumor formation, beyond the 2-month survival time point studied here (where no tumors were observed).

Concluding Remarks and Preclinical Relevance—In summary, we show here that Bcl-X$_L$ promotes the phenotypical stability of human fetal VM stem cells and renders them capable of generating mature SNpc DAn both *in vitro* and *in vivo*. From a mechanistic point of view, in addition to an efficient cell death counteraction, also described for human embryonic stem cells (21), Bcl-X$_L$ exerted a potent neuronal and DAn-inducing effect. Thus, combining an efficient cell death inhibition with an effective DAn induction could be an optimal way to obtain large amounts of genuine SNpc DAn from VM NSCs in the context of cell therapy for neurodegenerative disease, such as PD.

As exemplified in the present study and even when immortalized cell lines are not presently meant for clinical use, human VM cell lines represent a useful tool for the identification of key cellular and molecular processes that could be implemented in the future to obtain functional and healthy transplants. Also, human VM NSC lines are helpful research tools to obtain further insights in the molecular mechanisms of the human DAn induction and generation process. Last, gaining further mechanistic insights into Bcl-X$_L$ actions may help in the future to design pharmacological strategies to mimic its effects on hNSCs in the absence of a genetic modification.

Acknowledgments—We thank Dr. R. Moratalla (Cajal Institute, Madrid, Spain) for help with the behavior experiments and members of our laboratory and Prof. O. Lindvall (Lund University Hospital, Wallenberg Neuroscience Center, Sweden) for helpful comments on a previous version of the manuscript. We also thank Dr. P. Wiekop (NsGene A/S) for help with HPLC DA determinations, Dr. Ricardo Ramos (Scientific Park, Madrid, Spain) for help with Q-RT-PCR experiments, Dr. Piqueras and Dr. Cigudosa for help with karyotype analyses, and Dr. Smidt for providing the Pitx3 antibody. The excellent technical assistance of Beatriz Moreno, Inmaculada Ocaña, Bárbara B. Sese, Carlos Sánchez, Ignacio Tardieu, Isabel Manso, Juliana Sánchez, and Marta González is also gratefully acknowledged.

[6] I. Liste and A. Martínez-Serrano, unpublished data.

REFERENCES

1. Mendez, I., Viñuela, A., Astradsson, A., Mukhida, K., Hallett, P., Robertson, H., Tierney, T., Holness, R., Dagher, A., Trojanowski, J. Q., and Isacson, O. (2008) *Nat. Med.* **14,** 507–509
2. Winkler, C., Kirik, D., and Björklund, A. (2005) *Trends Neurosci.* **28,** 86–92
3. Christophersen, N. S., Meijer, X., Jørgensen, J. R., Englund, U., Grønborg, M., Seiger, A., Brundin, P., and Wahlberg, L. U. (2006) *Brain Res. Bull.* **70,** 457–466
4. Hedlund, E., Pruszak, J., Lardaro, T., Ludwig, W., Viñuela, A., Kim, K. S., and Isacson, O. (2008) *Stem Cells* **26,** 1526–1536
5. Lindvall, O., and Kokaia, Z. (2009) *Trends Pharmacol. Sci.* **30,** 260–267
6. Kim, H. J., Sugimori, M., Nakafuku, M., and Svendsen, C. N. (2007) *Exp. Neurol.* **203,** 394–405
7. Thompson, L., Barraud, P., Andersson, E., Kirik, D., and Björklund, A. (2005) *J. Neurosci.* **25,** 6467–6477
8. Lotharius, J., Barg, S., Wiekop, P., Lundberg, C., Raymon, H. K., and Brundin, P. (2002) *J. Biol. Chem.* **277,** 38884–38894
9. Storch, A., Paul, G., Csete, M., Boehm, B. O., Carvey, P. M., Kupsch, A., and Schwarz, J. (2001) *Exp. Neurol.* **170,** 317–325
10. Paul, G., Christophersen, N. S., Raymon, H., Kiaer, C., Smith, R., and Brundin, P. (2007) *Mol. Cell Neurosci.* **34,** 390–399
11. Caldwell, M. A., and Svendsen, C. N. (1998) *Exp. Neurol.* **152,** 1–10
12. Ostenfeld, T., Joly, E., Tai, Y. T., Peters, A., Caldwell, M., Jauniaux, E., and Svendsen, C. N. (2002) *Brain Res. Dev. Brain Res.* **134,** 43–55
13. Vila, M., and Przedborski, S. (2003) *Nat. Rev. Neurosci.* **4,** 365–375
14. Donato, R., Miljan, E. A., Hines, S. J., Aouabdi, S., Pollock, K., Patel, S., Edwards, F. A., and Sinden, J. D. (2007) *BMC Neurosci.* **8,** 36
15. Villa, A., Liste, I., Courtois, E. T., Seiz, E. G., Ramos, M., Meyer, M., Juliusson, B., Kusk, P., and Martínez-Serrano, A. (2009) *Exp. Cell Res.* **315,** 1860–1874
16. Boise, L. H., González-García, M., Postema, C. E., Ding, L., Lindsten, T., Turka, L. A., Mao, X., Nuñez, G., and Thompson, C. B. (1993) *Cell* **74,** 597–608
17. González-García, M., García, I., Ding, L., O'Shea, S., Boise, L. H., Thompson, C. B., and Núñez, G. (1995) *Proc. Natl. Acad. Sci. U.S.A.* **92,** 4304–4308
18. Shim, J. W., Koh, H. C., Chang, M. Y., Roh, E., Choi, C. Y., Oh, Y. J., Son, H., Lee, Y. S., Studer, L., and Lee, S. H. (2004) *J. Neurosci.* **24,** 843–852
19. Liste, I., García-García, E., Bueno, C., and Martínez-Serrano, A. (2007) *Cell Death Differ.* **14,** 1880–1892
20. Liste, I., García-García, E., and Martínez-Serrano, A. (2004) *J. Neurosci.* **24,** 10786–10795
21. Ko, J. Y., Lee, H. S., Park, C. H., Koh, H. C., Lee, Y. S., and Lee, S. H. (2009) *Mol. Ther.* **17,** 1761–1770
22. Villa, A., Snyder, E. Y., Vescovi, A., and Martínez-Serrano, A. (2000) *Exp. Neurol.* **161,** 67–84
23. Jensen, P., Bauer, M., Jensen, C. H., Widmer, H. R., Gramsbergen, J. B., Blaabjerg, M., Zimmer, J., and Meyer, M. (2007) *J. Neurosci. Res.* **85,** 1884–1893
24. Paxinos, G., and Watson, C. (1986) *The Rat Brain in Stereotaxic Coordinates*, 2nd Ed., Academic Press, Inc., New York
25. Jensen, J. B., and Parmar, M. (2006) *Mol. Neurobiol.* **34,** 153–161
26. Aruoma, O. I., Halliwell, B., Hoey, B. M., and Butler, J. (1989) *Free Radic. Biol. Med.* **6,** 593–597
27. Lotharius, J., Falsig, J., van Beek, J., Payne, S., Dringen, R., Brundin, P., and Leist, M. (2005) *J. Neurosci.* **25,** 6329–6342
28. Rawal, N., Parish, C., Castelo-Branco, G., and Arenas, E. (2007) *Cell Death Differ.* **14,** 381–383
29. Xu, J., Kao, S. Y., Lee, F. J., Song, W., Jin, L. W., and Yankner, B. A. (2002) *Nat. Med.* **8,** 600–606
30. Spector, S., Sjoerdsma, A., and Udenfriend, S. (1965) *J. Pharmacol. Exp. Ther.* **147,** 86–95
31. Kele, J., Simplicio, N., Ferri, A. L., Mira, H., Guillemot, F., Arenas, E., and Ang, S. L. (2006) *Development* **133,** 495–505
32. Yi, S. H., Jo, A. Y., Park, C. H., Koh, H. C., Park, R. H., Suh-Kim, H., Shin, I., Lee, Y. S., Kim, J., and Lee, S. H. (2008) *Mol. Ther.* **16,** 1873–1882
33. Smidt, M. P., Asbreuk, C. H., Cox, J. J., Chen, H., Johnson, R. L., and Burbach, J. P. (2000) *Nat. Neurosci.* **3,** 337–341
34. Rubio, F. J., Bueno, C., Villa, A., Navarro, B., and Martínez-Serrano, A. (2000) *Mol. Cell Neurosci.* **16,** 1–13
35. Morizane, A., Li, J. Y., and Brundin, P. (2008) *Cell Tissue Res.* **331,** 323–336
36. Chung, S., Shin, B. S., Hwang, M., Lardaro, T., Kang, U. J., Isacson, O., and Kim, K. S. (2006) *Stem Cells* **24,** 1583–1593
37. Villa, A., Navarro-Galve, B., Bueno, C., Franco, S., Blasco, M. A., and Martinez-Serrano, A. (2004) *Exp. Cell Res.* **294,** 559–570
38. Parsadanian, A. S., Cheng, Y., Keller-Peck, C. R., Holtzman, D. M., and Snider, W. D. (1998) *J. Neurosci.* **18,** 1009–1019
39. Savitt, J. M., Jang, S. S., Mu, W., Dawson, V. L., and Dawson, T. M. (2005) *J. Neurosci.* **25,** 6721–6728
40. Morrow, B. A., Roth, R. H., Redmond, D. E., Jr., Sladek, J. R., Jr., and Elsworth, J. D. (2007) *Exp. Neurol.* **204,** 802–807
41. Trouillas, M., Saucourt, C., Duval, D., Gauthereau, X., Thibault, C., Dembele, D., Feraud, O., Menager, J., Rallu, M., Pradier, L., and Boeuf, H. (2008) *Cell Death Differ.* **15,** 1450–1459
42. Stefanis, L. (2005) *Neuroscientist* **11,** 50–62
43. Hong, S., Kang, U. J., Isacson, O., and Kim, K. S. (2008) *J. Neurochem.* **104,** 316–324
44. Svendsen, C. N., Clarke, D. J., Rosser, A. E., and Dunnett, S. B. (1996) *Exp. Neurol.* **137,** 376–388
45. Chang, M. Y., Sun, W., Ochiai, W., Nakashima, K., Kim, S. Y., Park, C. H., Kang, J. S., Shim, J. W., Jo, A. Y., Kang, C. S., Lee, Y. S., Kim, J. S., and Lee, S. H. (2007) *Mol. Cell Biol.* **27,** 4293–4305
46. Haughn, L., Hawley, R. G., Morrison, D. K., von Boehmer, H., and Hockenbery, D. M. (2003) *J. Biol. Chem.* **278,** 25158–25165
47. Itoh, T., Itoh, A., and Pleasure, D. (2003) *J. Neurochem.* **85,** 1500–1512
48. Zhang, K. Z., Westberg, J. A., Hölttä, E., and Andersson, L. C. (1996) *Proc. Natl. Acad. Sci. U.S.A.* **93,** 4504–4508
49. Suzuki, A., and Tsutomi, Y. (1998) *Brain Res.* **801,** 59–66
50. Aouadi, M., Bost, F., Caron, L., Laurent, K., Le Marchand Brustel, Y., and Binétruy, B. (2006) *Stem Cells* **24,** 1399–1406
51. Duval, D., Trouillas, M., Thibault, C., Dembelé, D., Diemunsch, F., Reinhardt, B., Mertz, A. L., Dierich, A., and Boeuf, H. (2006) *Cell Death Differ.* **13,** 564–575
52. Alavian, K. N., Scholz, C., and Simon, H. H. (2008) *Mov. Disord.* **23,** 319–328
53. Martinat, C., Bacci, J. J., Leete, T., Kim, J., Vanti, W. B., Newman, A. H., Cha, J. H., Gether, U., Wang, H., and Abeliovich, A. (2006) *Proc. Natl. Acad. Sci. U.S.A.* **103,** 2874–2879
54. Andersson, E. K., Irvin, D. K., Ahlsiö, J., and Parmar, M. (2007) *Exp. Cell Res.* **313,** 1172–1180
55. Albéri, L., Sgadò, P., and Simon, H. H. (2004) *Development* **131,** 3229–3236
56. Sun, Y., Nadal-Vicens, M., Misono, S., Lin, M. Z., Zubiaga, A., Hua, X., Fan, G., and Greenberg, M. E. (2001) *Cell* **104,** 365–376
57. Fernando, P., and Megeney, L. A. (2007) *FASEB J.* **21,** 8–17
58. Fernando, P., Brunette, S., and Megeney, L. A. (2005) *FASEB J.* **19,** 1671–1673
59. Khan, Z., Akhtar, M., Asklund, T., Juliusson, B., Almqvist, P. M., and Ekström, T. J. (2007) *Exp. Cell Res.* **313,** 2958–2967
60. Geeta, R., Ramnath, R. L., Rao, H. S., and Chandra, V. (2008) *Biochem. Biophys. Res. Commun.* **373,** 258–264